Theoretical Proof Of Concept For The Green Revolution Energy Converter

Development of a mathematical model, material analysis and physical model improvements

---

Institution: IEI

Markus Eriksson
Markuseriksson.lkpg@gmail.com

Oscar Magnusson
oscma067@student.liu.se

Lukas Haglund
lukha790@student.liu.se

John Malmdal
johma836@student.liu.se

Gustav Edholm
gused621@student.liu.se

2022-03-25

LINKÖPINGS UNIVERSITET

Abstract

The GREC is a new type of renewable heat engine that challenges the current dominating combustion engines. By using renewable energy the GREC offer a theoretical high efficiency, possibilities for large scalability and a high power output. The GREC could therefore be a step into a better future regarding energy production without consumption of fossil fuel. The report has the aim to further develop the fundamental technology and present a theoretical proof of concept of the GREC engine. This was performed by establishing a mathematical model in order to produce realistic results in terms of performance. As well as material analyzes and construction improvements of crucial parts for future physical models.

The mathematical model was constructed with the help of the fundamental principals of the Carnot-engine. With this in mind the development of the mathematical model was formed by stating necessary thermodynamic assumptions, equations and simplifications that focused on the heat transfer within the engine. The material analysis focused on performing thermal and stress simulations on selected parts with sought out material properties that would benefit the efficiency for the GREC. With the use of a scaled Six Sigma quality approach future construction improvements could be pinpointed and thereby give guidance to future work.

Results show that the GREC theoretically benefits performance-wise by being constructed in larger scales and with higher temperature differences between two heat reservoirs. Change of construction materials also show increased performance, for example using bakelite for isolation. The found construction improvements using Six Sigma across the physical model show that a path to a solution of the problem could be pinpointed. This will also contribute to GRECs development when solved.

Acknowledgement

We would like to express a special thanks of gratitude to Nils Karlberg, the innovator of the GREC, as well as Sophia Karlberg, CEO of nilsinside AB. These two gave us the golden opportunity to learn more about this project and have throughout this report been a continuous support with lots of energy. We are certain that the knowledge we have gotten from this project will help us in our journeys to become engineers.

Contents

Nomenclature

Symbol	Parameters	Unit
$P_{segment}$	Perimeter of segment	m
d_h	Hydraulic diameter of segment	m
r	Radius	m
$r_{air\,space}$	Radius of the air space between RS and the conducting fin	m
L	Arc length	m
$t_{segment}$	Thickness of segment	m
$w_{segment}$	Width of segment	m
$A_{segment}$	Area of segment	m^2
z	Height coordinate	m
v	Tip speed	m/s
n	Rotation per minute	rpm
f	Frequency	Hz
m	Mass	kg
V	Volume	m^3
T_h	Temperature of conducting fin (Warm side)	°C
T_c	Temperature of conducting fin (Cold side)	°C
p_{1-4}	Pressure	Pa
W	Work	J
Q	Heat energy	J
u	Specific internal energy	$\frac{J}{kg}$
$\dot{W}$	Power	W
$\dot{Q}$	Heat	W
R	Specific gas constant	$\frac{J}{kgK}$
c_v	Specified heat capacity (Constant volume)	$\frac{J}{kgK}$
c_v	Specified heat capacity (Constant pressure)	$\frac{J}{kgK}$
k	Thermal conductivity	$\frac{W}{mK}$
h	Heat transfer coefficient (HTC)	$\frac{W}{m^2K}$

Greek Symbols

Symbol	Parameters	Unit
μ	Dynamic viscosity	$\frac{kg}{m^3 s}$
ρ	Density	$\frac{kg}{m^3}$
ω	Rotation velocity	rad/s
η_{th}	Thermal efficiency	%
η_{tot}	Total efficiency	%
$\eta_{Carnot,th}$	Carnot efficiency	%

Dimensionless numbers

Symbol	Parameters	Unit
Re	Reynolds number	[N/A]
Pr	Prandtl number	[N/A]
Nu_t	Nusselt number (Turbulent flow)	[N/A]
Nu_l	Nusselt number (Laminar flow)	[N/A]

1 Introduction

There is no question today regarding the relevancy of the climate crisis and that it is in dire need for a change in the right direction [1]. If we are to prevent global warming from exceeding 1,5 degrees, there is a need for innovative solutions which must be carried out in the next upcoming years. One of these potential solutions is "The Green Revolution Energy Converter" (GREC), under development by nilsinside AB and is patented internationally since 2013 [2]. The GREC has the potential to change the future in both the sector of energy production as well as in the sustainable transport sector.

1.1 Background

The GREC is a heat engine, redefined in a way that has never been done before. A heat engine is a motor which can transform temperature gradients into mechanical power by utilizing the pressure changes which occur when a closed volume of gas (later referred to as the Work Generating Volume) alternately is warmed up and cooled down. The pressure changes cause the volume to expand and retract which in turn can allow a piston to move back and forth, thus producing mechanical work. This thermodynamic concept can be compared to a Stirling-engine, which theoretically can match the efficiency of a theoretical Carnot-engine. The Stirling-engine is however not feasible for large scale energy production due to its poor power-to-weight ratio, resulting in poor scalability. The GREC on the other hand is not just any heat engine, what makes the GREC so unique is primarily its potential for large scalability and variable speed. In addition to this the GREC is also low cost, zero emissions and very flexible in terms of applications use.

The development of the GREC is still in its early stages and lies on a Technology readiness level (TRL) of 3-4 on a total scale of 9. The Technology Readiness Level is a type of measurement system used to assess the maturity of a particular technology and the TRL-value describes which phase the development of the technology currently is at [3]. Level 1 translates to the initial stage where the basic principle of the technology is observed, and level 9 translates to the final stage where the technology is totally proven in an operational environment and a competitive manufacturing alternative on the market. At level 3-4, an experimental proof of concept must be carried out in order to proceed into further validation of the concept in relevant environments (such as industrial environments).

1.2 Technology of the GREC

The GREC can be thought of as a revolving Carnot-engine which means that the Work Generating Volume (WGV) is continuously rotating from a warm source to a cold source, transferring its heat from the respective source when in contact. The WGV is pushed around by a rotating disc mounted on a shaft, called the Revolving Shutter (RS). A quarter opening is included in the RS which holds the WGV. The rotation of the RS is powered by an electric motor which in turn is controlled by software that can adjust the speed of the RS, allowing for a variable speed and power output in accordance with the current state of the environment. Insulating the how and cold sources from each other and containing the WGV is done by two insulation blocks called Nil blocks which are placed in between the warm and the cold block see figure (1). When the electric motor rotates the RS holding the WGV, it can be understood that the pressure will rise when the WGV is in contact with the warm source which transfers its heat to the WGV. The opposite effect occurs when the WGV is in contact with the cold source, meaning that the pressure drops since the WGV transfers its heat to the cold source. Then the procedure repeats itself, allowing pressure pulses and therefore work to be created at the speed of which the RS is rotating [4].

It is important to understand that the RS, heat source- and insulating blocks all are built up in layers, or fins. Consequently, this means that the WGV also becomes a column of sliced volumes in between each layer of fins of the surrounding blocks, see figure (1). Thinly sliced columns of gaseous volume results in a significantly higher heat transfer rate from the heat source fins to the WGV, which is a key property for the GREC. The amount of layers can be selected at will when constructing the GREC since this entails the WGV capacity and therefore the maximum potential power output [4].

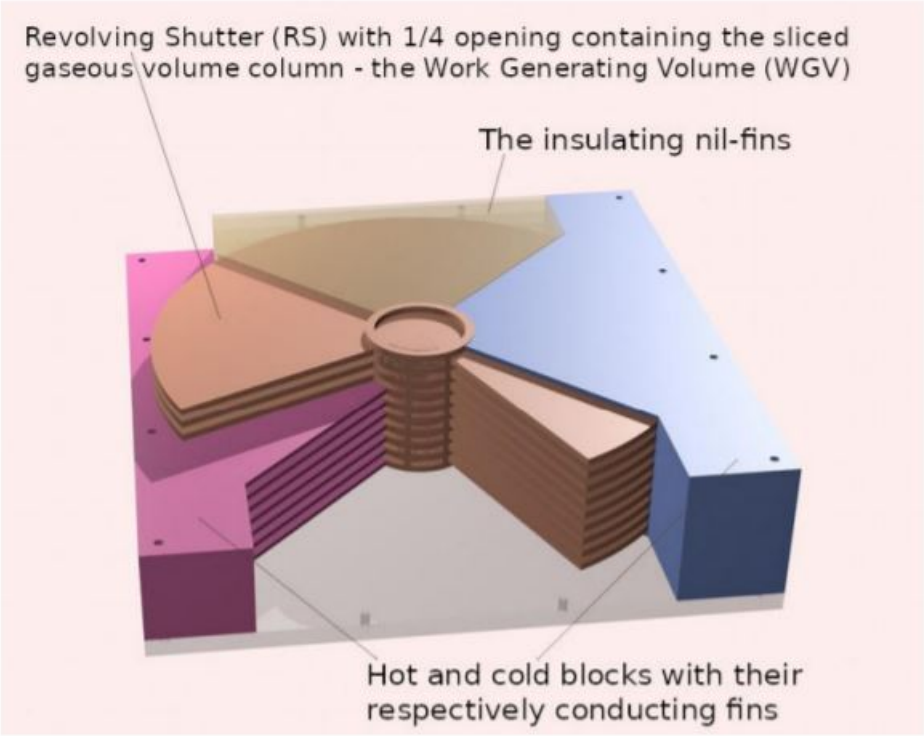

Figure 1: A schematic sectional view of the GREC with text reference for different parts [5].

1.3 Aim

The possibilities of the GREC concept are wide and could revolutionize the heat engine perspective for future appliances. With the incentive for an affordable and clean green energy source, the GREC's heat transfer technology could be a opportunity regarding both economic growth and tackling climate change. Its use range from appliances in the industry sector to geothermal motors or in the process of energy storing. It could also be utilized in our everyday life within the transport sector (eg. bus-transportation). By using the GREC technology with a green heat source you can produce renewable energy without the dangerous substances that all heat engines use today. With all these possibilities in mind the interest of GREC's green technology enormous potential regarding the UN's Sustainable Development Goals [6]. Consequently the GREC could be seen as the replacement of the existing polluting nonrenewable heat engines.

1.4 Objective

The primary objective in this project is to carry the overall GREC-project forward by verifying the fundamental aspects of which the GREC-concept relies on. The primary objective can be divided into the following sub-objectives:

- Create a system of mathematical models which will enable to verify the theoretical "proof of concept" of the GREC.
- Carry out material analyzes for crucial parts regarding isolation and heat transfer properties.
- To analyze and pinpoint construction improvements on the physical model that should improve future models of the GREC.

1.5 Questions to be answered

- Does the mathematical model system prove a realistic and a clarification for the "proof of concept"?
- How does scaling the model affect the performance?
- Regarding the material analysis, which materials are the most preferred for the crucial parts for the usage of GREC?
- What are the pinpointed construction improvements for future models?

1.6 Limitations

In order to complete the objectives and therefore moving the GREC concept towards the aim of the study, some limitations have been adopted both before the start as well as during the experiments. The limitations are as follows:

- The physical model is delivered from Nilsinside AB, therefore we have not been part of any construction, measuring or material choices.
- After a lot of time spent on problem solving the physical model, we can clarify that the physical model has a considerable malfunction inside the engine that makes the operation drift fail. therefore the physical model can not be considered to be any sort of comparison for the theoretical mathematical model system.
- The simulation model will correspond to the physical model, meaning that the simulation model will consist of the same amount of layers, measurement, size, temperature and etc.
- We will provide new scenarios within the simulation area in terms of new materials, focusing only on the crucial parts as mentioned in objectives therefore some material parts will not be analyzed.
- Fluid-simulations and accurate calculations of properties within the turbulent WGV will not be performed in the system of mathematical models.

2 Theory

2.1 Equations

The following equations are represented and used in a mathematical calculation program called MATLAB. However more ongoing explanations of the program will be more in detail in the forthcoming chapters. Equations (1) - (9) are basic dimension analysis equations, however equation (10) - (26) can be found in the following source [7].

The angular velocity for the rotating shutter.

$$\omega = \frac{n2\pi}{60} \tag{1}$$

Arc length

$$l = r\pi \tag{2}$$

Cross-sectional area for each segment

$$A_{segment} = w_{segment}\, t_{segment} \tag{3}$$

The perimeter of the cross-sectional for each segment

$$P_{segment} = 2w_{segment} + 2t_{segment} \tag{4}$$

The velocity for the air

$$v = \omega r \tag{5}$$

The resulting power depending on the amount of work and frequency of the rotating shutter

$$\dot{W} = Wf \tag{6}$$

The compiled radius for the WGV.

$$WGV_{radius} = r_{RS} + r_{air\,space} - r_{RS\,shaft} \tag{7}$$

Calculation of the WGV for the whole engine.

$$WGV = \frac{\pi(r_{RS}^2 - r_{RS\,shaft}^2 + r_{air\,space}^2)}{4} \cdot Shell\,thickness \cdot Level \tag{8}$$

The time it takes for the WGV to make a half rotation

$$t = \frac{0.5}{f} \tag{9}$$

The ideal gas law.

$$pV = mRT \tag{10}$$

The hydraulic diameter which is the characteristic length for a non-circular pipe.

$$d_h = \frac{4A_{segment}}{P_{segment}} \tag{11}$$

Reynolds number

$$Re = \frac{\rho v k}{\mu} \tag{12}$$

Prandtl number

$$Pr = \frac{c_v \mu}{k} \tag{13}$$

The Nussel number for laminar flow at forced convection in a pipe.

$$Nu_l = 3,65 + \frac{0,067 RePr\frac{d_h}{L}}{1 + (0,04(RePr\frac{d_h}{L})^{\frac{2}{3}})} \tag{14}$$

The Nussel number for a turbulent flow at forced convection in a pipe.

$$Nu_t = \frac{0,038 Re^{\frac{3}{4}} Pr}{1 + (1,5 Re^{-\frac{1}{8}} Pr^{-\frac{1}{6}} (Pr - 1))} \tag{15}$$

Heat transfer coefficient.

$$h = \frac{kNu}{d_h} \tag{16}$$

Newtons heat transfer law.

$$\dot{Q} = hA(T_h - T_{WGV}) \tag{17}$$

The first law of thermodynamic for a closed system.

$$Q = m(u_2 - u_1) + \frac{1}{2} m(v_2^2 - v_1^2) + mg(z^2 - z^1) + W_{12} \tag{18}$$

Calculation of the change internal energy, with the temperature difference and c_v.

$$u_2 - u_1 = c_{v,air}(T_2 - T_1) \tag{19}$$

A simplified versions of equation (18), where the kinetic and potential part is neglected and the change of internal energy was calculated with equation (19).

$$Q = mc_{v,air}(T_2 - T_1) \tag{20}$$

The resulting work from the change of volume.

$$W_{12} = p_1 V_1 ln\frac{V_2}{V_1} \tag{21}$$

The net power out.

$$W_{net,out} = W_{exp} - W_{comp} \tag{22}$$

Thermal efficiency.

$$\eta_{th} = \frac{W_{net,out}}{Q_H} \tag{23}$$

Thermal efficiency.

$$\eta_{th} = 1 - \frac{\dot{Q}_c}{\dot{Q}_H} \tag{24}$$

Carnot efficiency.

$$\eta_{th} = 1 - \frac{T_c}{T_H} \tag{25}$$

Total efficiency.

$$\eta_{tot} = \frac{\dot{W}_{net,out} - \dot{W}_{in}}{\dot{Q}_H} \tag{26}$$

2.2 Heat engines

In thermodynamics, a heat engine is a system that is able to do a conversion of thermal energy or heat to mechanical work[8]. It does this by a principle of moving a working substance from an higher temperature area to a lower temperature area and then operate in a cycle. A simplified heat engine visualization can be seen in figure (2). Even though the principle of the heat engine sounds simple the true understanding of the use of energy transfer by heat was as late as in the middle of the nineteenth century [9]. This discovery lead to three different heat transfer mechanisms, conduction, radiation and convection. The last one, convection, is of the most important and the focus for heat engines due to the transfer of energy between a solid surface and the adjacent working substance that are in motion, this is a combined effect of conduction and fluid motion.

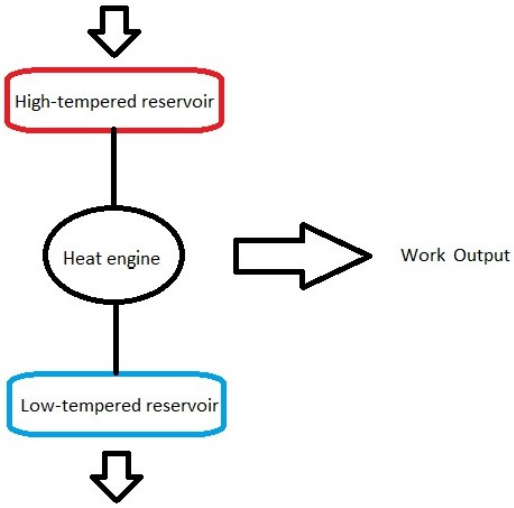

Figure 2: Heat engine.

The understanding of heat engines comes from the first and second law of thermodynamics[10]. The statement for the first law is that the total energy of a system remains constant, even if there is a phase converting between themselves. This law is often called the conservation of energy and can be described by this example: the energy that a car has when it moves, kinetic energy, is converted to heat energy when the driver presses the brakes on the car to slow it down. The first law of thermodynamics introduces the variable enthalpy, which is connected to temperature. The definition of the law itself allows for processes to exist but experience indicates that only certain states occur as energy can certainly be transferred from one place to another. This leads on to the second law and the variable, entropy. The second law can be stated in various forms that may seem different but are in fact all the same. As this law gives overall insight into how nature works and therefore broadly applicable and highly fundamental for many processes. This second law is therefore a sort of judge that decide whether the process will occur or not. So in terms of the process that will occur in a heat engine the first and second law of thermodynamic need to be fulfilled.

As pointed out in the example with the breaking car, work can be converted to other forms of energy but converting energy to mechanical work is not that easy. Heat engines are cyclic driven and are in need of a working substance that will be transferred during the cycle[10]. The working substance can either be liquid, air or gas. If the working substance is implemented into the heat engine and is heated up so all the contained heat is converted to work. By definition it will then be released to the environment with zero absolute temperature, which is the lowest theoretical temperature, or with no heat. Since this is impossible considering the two thermodynamic laws [9], the heat engine therefor need two different heat reservoirs as implemented in figure (2). The principle is that one reservoir is a provider of the heat and the other one absorb the working substance after the extracting work. So by implementing the two thermodynamic laws

there must be a high-tempered reservoir that can provide heat and a low-tempered reservoir that can receive the work that has been performed. This leads on to the Kelvin-Planck statement[9]:

> "It is impossible for any device that operates on a cycle to receive heat from a single reservoir and produce a net amount of work"

This statement correlates with the heat engine since it cannot work fully ideal. therefore there is always a limitation regarding the thermal efficiency of heat engines since it must exchange heat with a lower-tempered reservoir as well as an high-tempered source to operate. But note that the Kelvin-Planck statement cannot be proven theoretically, a negation which has been determined by experiments when considering the first law. Then one may ask, how do we find the most efficient engine possible given two heat reservoirs. To define this question the knowledge of the concept of reversibility must be quantified.

2.2.1 Irreversibilities

A reversible process is simply one that, once it has taken place, can be reversed back to the original state[10]. As said before regarding the non realistic zero absolute temperature, this is only possible if the heat and work exchange between the surrounding and the system is non existing. Processes that are not reversible are called irreversible processes. The factors that cause the process itself to be irreversible are called irreversibilities [9]. This include the following factors:

- Friction losses; Associated with bodies in motion, when bodies slide across each other energy is lost because some work is needed to overcome the force acting like friction. Energy loss also occur when the process is reversed. The larger the friction, the more irreversible the process is.
- Heat transfer across a finite temperature difference; This irreversibility means that when drop in finite temperature in a process is reversed the heat transfer from a low-tempered reservoir to a high-tempered reservoir, this is thermodynamic impossible.
- Unrestrained expansion of a gas; A gas cannot be compressed to a state without doing work or heat being applied.
- Mixing of simple substances; When mixing substances applied work is required to separate, this type of process cannot be reversed.
- Chemical or nuclear reactions; When a nuclear or chemical reaction has occurred the initial products cannot be converted back without the input of energy.

2.2.2 Carnot cycle

As mentioned, heat engines are cyclic and that the working substance in the engine returns to the initial state at the end of each the cycle. When considering only reversibility, the most known is the Carnot heat engine that first introduced in the early eighteen hundreds by the French engineer Sadi Carnot[9]. This engine uses reversible processes to complete a thermodynamic cycle and produce the most useful work possible [10]. The Carnot heat engine has therefore become a sort of standard which other heat engines can be compared and compete against with the use of thermal energy available in a high-temperature reservoir.
A simplified version of the Carnot heat cycle can be seen in figure (3), is composed of four reversible processes [9] [10] and with help of a adiabatic piston-cylinder containing a gas it can illustrate the whole cycle:

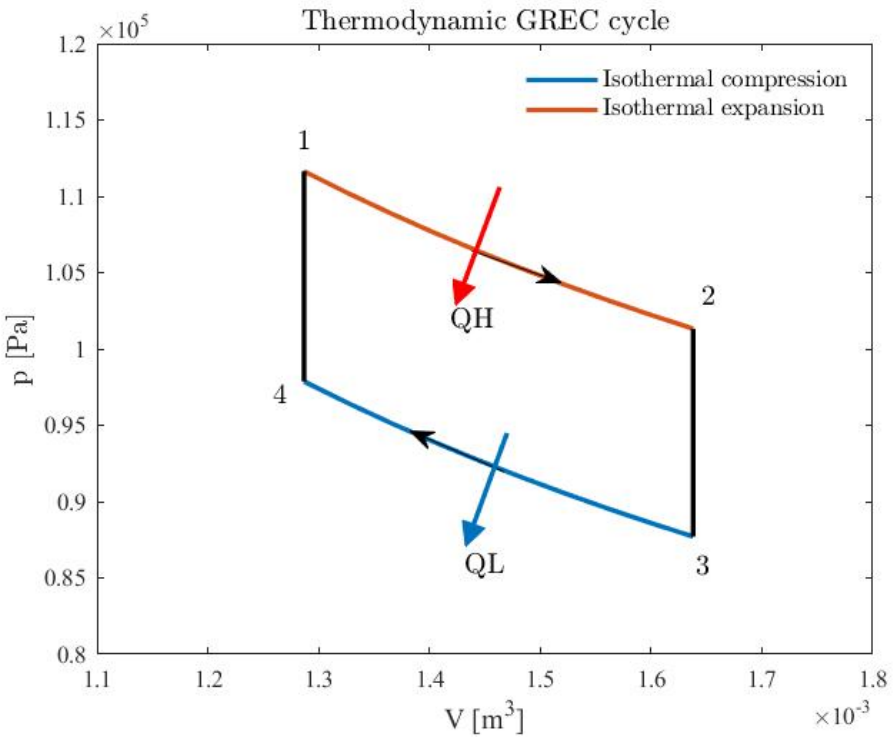

Figure 3: Illustration of how a p-V diagram of the GREC cycle can look like.

1. **Reversible Isothermal Expansion 1-2**
   Initially , the energy source T_H is constant as seen in figure (4). This will then affect the gas in the closed cylinder that will strive to reach T_H. In addition, the cylinder head will then be in contact with the energy source T_H(High-tempered reservoir). Next, the gas will be allowed to expand slowly doing work on its surroundings. Note that when the cylinder head is moving there will be a drop in the temperature in the closed cylinder. Since the transfer of T_H is occurring slowly, the source T_H will transfer heat back into the cylinder keeping it constant. This continues until the piston head reaches state 2. The total heat amount of heat transferred to the gas during this process is Q_H.

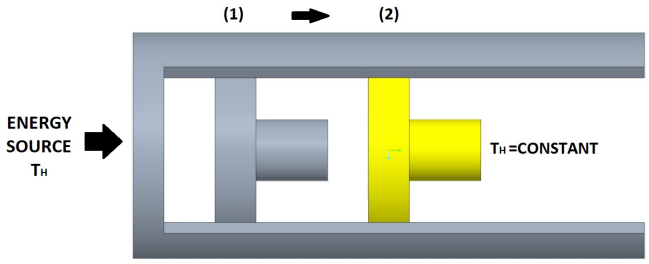

Figure 4: Process 1-2.

2. **Reversible Adiabatic Expansion 2-3**
   During this expansion seen in figure (5) the temperature will drop from T_H to T_L(low-tempered reservoir). The reservoir that was in contact with the cylinder head will then be replaced by an insulation and the system becomes adiabatic. State 2 will then be slowly moving to state 3 as the gas continues to expand doing work on its surroundings until it reaches state 3 when the drop in temperature has been made. The piston is assumed to be frictionless and the process to be quasi-equilibrium[11].

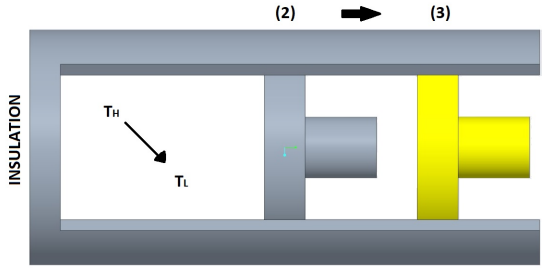

Figure 5: Process 2-3.

3. **Reversible Isothermal Compression 3-4**
   In this compression seen in figure (6) T_L is constant. The insulation at the cylinder head is removed and will be replaced with a sink that is at a temperature T_L. When the sink is introduced the piston will be pushed inward by an external force that will be doing work on the gas. The gas then will be compressed and its temperature will therefore rise. However as the temperature rises the amount of heat will be transferred into the sink causing the gas temperature to drop to T_L at state 4. The total amount of heat rejected from the gas during this process is Q_L.

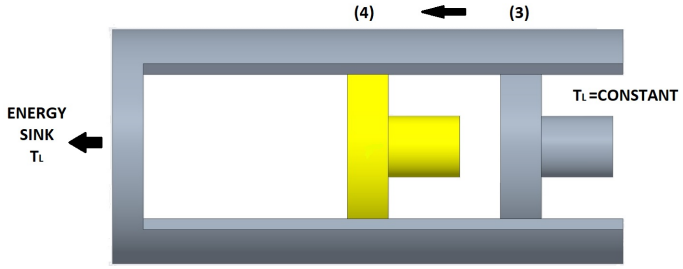

Figure 6: Process 3-4.

4. **Reversible Adiabatic Compression 4-1**
   Finally the last compression seen in figure (7) will be compressed in a reversible manner as state 1-2. Here the sink(low-tempered reservoir) will be replaced with a insulation that yet again will put back the cylinder head and the gas will be compressed and return to its initial state 1 and the Carnot cycle is completed.

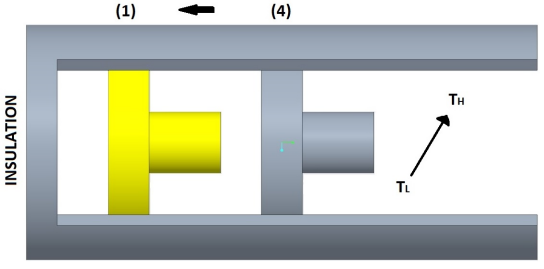

Figure 7: Process 4-1.

2.3 GREC concept

A process within Thermodynamics is defined as "any change a system undergoes from one equilibrium state to another" [9]. It's important to know what processes a system contains and how they relate to each other in order to understand how a heat engine works in real life. As previously mentioned in the heat engine chapter, the GREC can be thought of as a revolving Carnot-cycle. The Carnot-cycle consists of four working processes, Isothermal expansion, adiabatic expansion, Isothermal compression and adiabatic compression, see figure (3). Even though the Carnot-cycle only is applicable in theory and impossible to recreate in real life, it can still be used to translate and interpret the functionality of the GREC. The GREC is built in four separate sections, and each section can be thought to fulfill each respective working process in a Carnot-cycle. To understand how the sections relate to the working processes, a full cycle within the GREC connected to an external piston will be explained in detail, see figure (8).

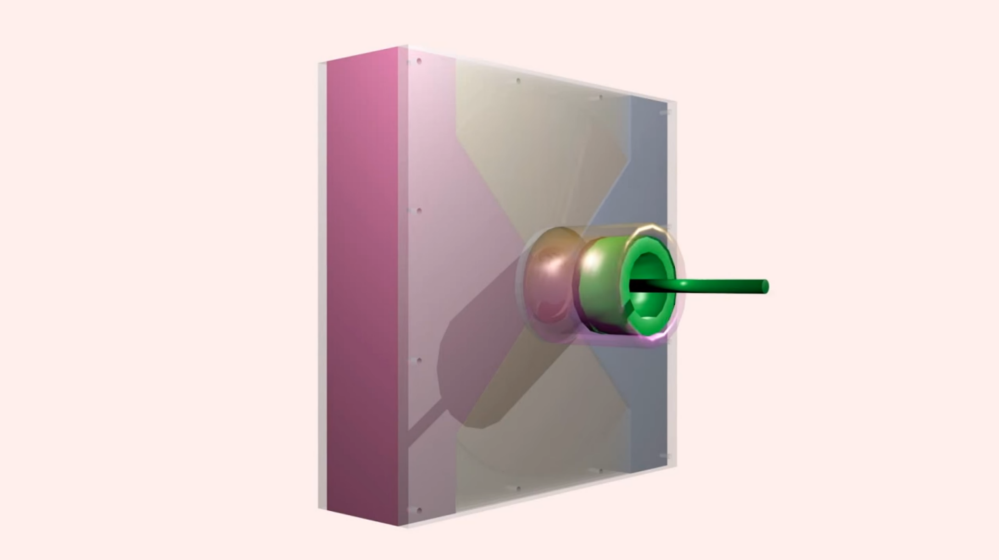

Figure 8: A schematic view of the GREC connected to an external piston [5].

When the WGV rotates and makes initial contact with the hot source, see figure (9a), heat energy is transferred to the WGV which causes the temperature and pressure to rise fast. As a result, the WGV is forced to expand, causing the externally connected piston to be pushed upwards, thus producing work. While the volume expands, the pressure drops but the temperature stays relatively the same, see process 1-2 in figure (3) and compare to the Isothermal expansion (constant temperature expansion) in the Carnot-cycle. The Isothermal expansion process endures until the WGV no longer receives heat from the hot source and only is in contact with the neutral insulation, see figure (9b).

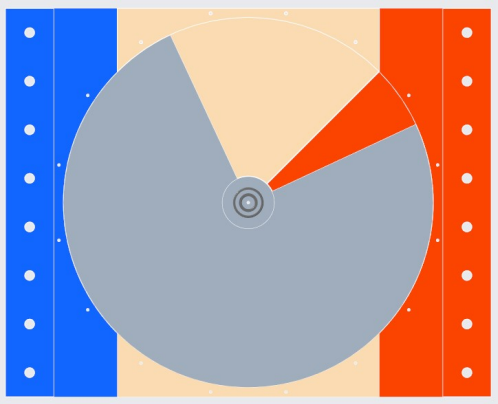

(a) The WGV enters the warm source.

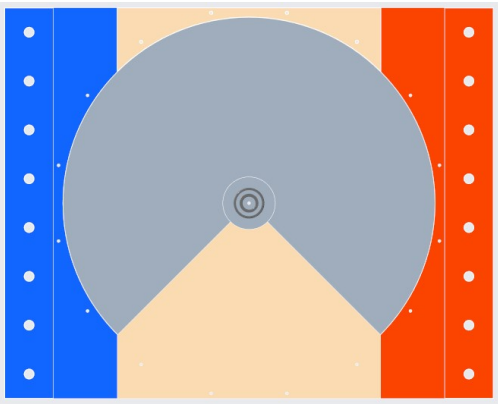

(b) The WGV is isolated between both sources.

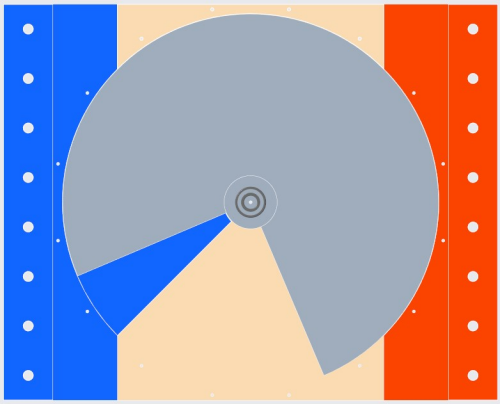

(c) The WGV enters the cold sink.

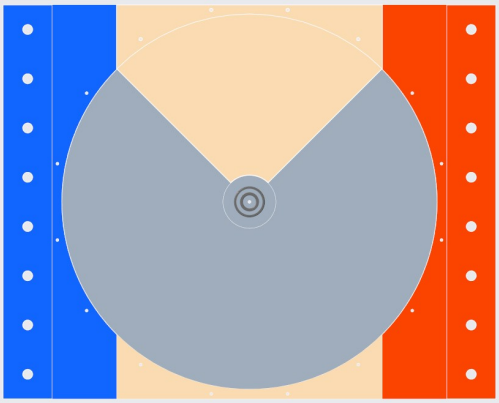

(d) The WGV is isolated between both sources.

Figure 9: A visualization of one revolution of the rotating shutter (RS), presented in 4 instantaneous states. The direction of rotation is clockwise and the blue and red section represents the cold sink and the warm source respectively.

The neutral insulating section of the GREC has two purposes. Firstly it is used to separate the hot source from the cold sink and make sure that the WGV never can be in contact with both sources at the same time which would affect the efficiency immensely. Secondly it is used to eliminate a large volume of gas which is not included in the WGV. Gaseous volume inside the GREC which is not contained within the quarter of the RS is considered "dead volume". Where the dead volume is defined in the model is illustrated in figure (10). Dead volume has a negative effect on the efficiency of the GREC since this volume simultaneously can be heated up and cooled down which is not ideal for efficiency. During the moment where the WGV is completely isolated from both heat sources, little to no heat is supposed to be transferred to or from the WGV. However, the volume still expands a bit more and therefore pushes the piston further while the temperature and pressure drops due to that there is no added heat. These moment of events can be related to the adiabatic expansion process in the Carnot-cycle.

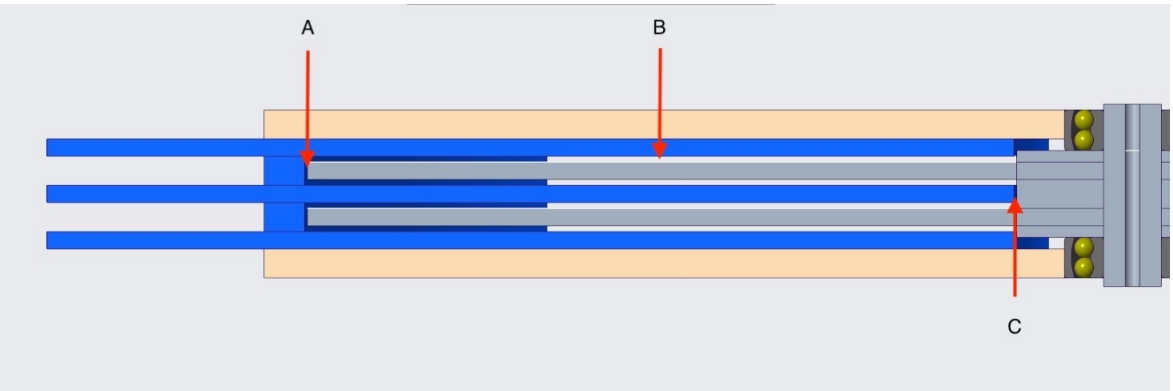

Figure 10: A schematic view of where the dead volume is defined. (A) is the airspace between the revolving shutter and the surrounding wall. (B) is the airspace between revolving shutter and the conducting fin and the last place is (C) is a airspace located between the conducting fin and the shaft of the revolving shutter.

When the WGV enters the cold side in figure (9c), the WGV transfers its heat to the cold sink, causing the pressure and temperature to drop quickly. The pressure inside the WGV drops below the atmospheric pressure, thus pushing the piston down again and compressing the volume. While the WGV compresses, the pressure starts to rise again and the temperature stays more or less constant since heat from the WGV is disposed of simultaneously. This process can be related to the Isothermal compression process in a Carnot-cycle and it will proceed until the WGV is completely isolated from both heat sources, likewise to the Isothermal expansion.

The WGV has now rotated to the last section in the GREC which is the second insulation quarter, see figure (9d). Yet again, no heat is ideally to be transferred in or out from the WGV while it is continuing to compress further, and therefore causing the pressure and temperature to increase. This last step which also completes the revolution of the cycle can be compared to the adiabatic compression process in a Carnot-cycle.

2.4 Losses in the GREC

A statement from the second law is "Clausius" statement which implies that natural spontaneous processes only occurs in the direction from a warm to cold body and not the other way. This also suggests that reversible processes can't occur naturally and only can be approximated by actual devices, implying that a fully reversible process doesn't exist. The irreversibilities can be linked together with the losses of energy in the system. therefore, irreversibilities and losses are important to localize to determine the feasibility and efficiency of the engine. There are 3 primary types of losses in the GREC listed and explained below.

1. **Heat losses**

   Since no heat engine can be a hundred percent efficient, it is understood that the amount of added heat energy to a system cannot be fully converted to the equivalent amount of work, meaning that remaining energy is disposed of from the system as waste heat. Equation (23) says that the thermal efficiency of a heat engine is equivalent to the net work output divided with the total amount of added heat energy, it can also be expressed as equation (24). In addition to this Carnot found that for a reversible engine the ratio in heat energy between two reservoirs is the same as the ratio in absolute temperature, thereby obtaining equation (25). This equation yields the maximum theoretical thermal efficiency for a reversible heat engine and suggests that a lower temperature gradient decreases the efficiency and therefore is a loss itself. Notice that this maximum efficiency cannot be achieved by the GREC since it is not entirely reversible, but the expression still acts like a reference roof for what to expect.

In the GREC both the insulation and the rotor module are supposed to absorb as little heat as possible from the heat source and gaseous volume, since all heat that escapes past the WGV isn't contributing to the net work output. Therefore this is a heat loss that is dependent on choice of material. Since the material should be isolating and not absorb any heat, it needs to have certain qualities. It should have low heat capacity, c_p and low heat-transfer rate, k. This means that the material for the RS will not transfer any heat from the hot side to the cold side. If the RS would transfer heat between the two sides, the pressure ratio would drop and less work would be put out.

If these specific components have the material qualities as mentioned above, the overall efficiency will increase since the main portion of the heat will be absorbed by the WGV.

2. **Mechanical friction losses**

   Since the RS revolves around a bearing shaft powered by an electric motor, some friction between the shaft and bearings is likely to occur even though it would be minimal, nonetheless it is a loss in the system. The externally connected pressure-operated device which converts pressure to work will also cause irreversibilities affecting the total efficiency of the GREC. As mentioned earlier friction causes irreversibilities, take a cylinder with a moving piston for example. Contact between the moving piston and cylinder creates a friction force opposite to the moving direction. Since this force must be vanquished, additional work is needed for the piston to move. The energy supplied as work to overcome the friction is eventually converted to heat and transferred to the bodies in contact, that is the cylinder and piston. Heat produced due to friction is a loss and decreases the generated amount of net work.

3. **Fluid friction losses**

   Friction can also emerge when a solid body in motion comes in contact with a fluid or gas, so called drag. Drag is generated by the difference in velocity between the solid body and the fluid and acts in the direction that opposes the motion [12]. When the fluid moves and achieves a certain velocity, fluid resistance forces occurs and this is measured with a Reynolds' number. A larger Reynolds number means a more viscous fluid flow, and is calculated with equation (12). If Reynolds number is greater than 2300 this implies the flow is turbulent and laminar if the respective value is lower than 2300 [7]. Drag might be thought to only have a negative impact in most applications since it drains energy which is true for a majority of cases. However, the GREC actually desires drag since it creates a turbulent flow which achieves a relatively higher heat transfer coefficient compared to a laminar flow. A higher heat transfer coefficient in the WGV increases its capacity to absorb and dispose of heat which enables the GREC to produce larger pressure pulses and thereby more power. Turbulence emerges only in the gaseous volume within the quarter opening (WGV) of the RS, while the layers of gaseous "dead volume" between each layer of fins and rotor-discs becomes laminar. This is beneficial because the laminar flow between the fins and rotor-discs helps to both reduce friction and unwanted heat transfer between the WGV and other materials. Even though the dead volume has benefits, it should still be minimized since it consumes power and cannot be utilized to produce pressure pulses as efficiently.

2.5 Material selection

The choice of materials in a heat engine are important. Rotating parts must be stiff in order to prevent large elastic deformation and lightweight to move without too much resistance. The thermal properties are also important to consider in a environment where high temperature differences occur. Since rotating parts in engines often operate within a narrow tolerance area, the material must therefore be resistant to thermal deformation. The rotating disc in this project rotates between a warm and a cold side and must therefore be heat resistant. The reason for this is to keep the heat to the warm side, and the cold to the cold side. Otherwise the pressure difference would be lowered hence decreasing the overall efficiency.

Applying knowledge of thermal insulation, which is the reduction of heat transfer when objects are in thermal contact, isolation materials has a great potential to increase the thermal energy conservation in the engine [13]. With this in mind the relevance for choosing right material for the technology of the GREC is important since heat transfer is central . Material qualities are described by heat capacity, c_p and heat-transfer rate, k.

Meanwhile thermal conduction is the ability to transfer heat [13]. This imply to conduct or emit heat at a high rate to in this case establish great temperature- and pressure differences, which is needed in a heat engine. This requires the opposite material qualities compared to the isolating module. Hence to have a high heat capacity and high heat-transfer rate is needed to achieve these qualities.

---

3 Method

In this chapter the approach of the project will be explained. It will include how the experiments were conducted, how the calculation model was developed in MATLAB, the construction of simulation in ANSYS and the CAD model in CREO. Measures for improvements of the GREC are also presented.

3.1 Establishment of mathematical models

The theoretical calculation model was constructed to visualize the capabilities of the physical GREC-model and with that make an overall assumption for key parameters. The dimensions of the standard mathematical GREC model are retrieved from the dimensions of the physical model. The values of these dimensions are presented in table (1). How the parameters are defined is displayed in figure (11) and (12).

Table 1: Dimensions of the physical GREC-model and the parameters that were used in the MATLAB-software.

Dimension/Parameters	Value	Unit
Length	0,6	[m]
Width	0,6	[m]
Conducting fin thickness	0,006	[m]
Revolving shutter thickness	0,006	[m]
Shell thickness	0,007	[m]
Case thickness	0,006	[m]
Radius rotor	0,29	[m]
Radius shaft	0,04	[m]
Levels	2	[N/A]

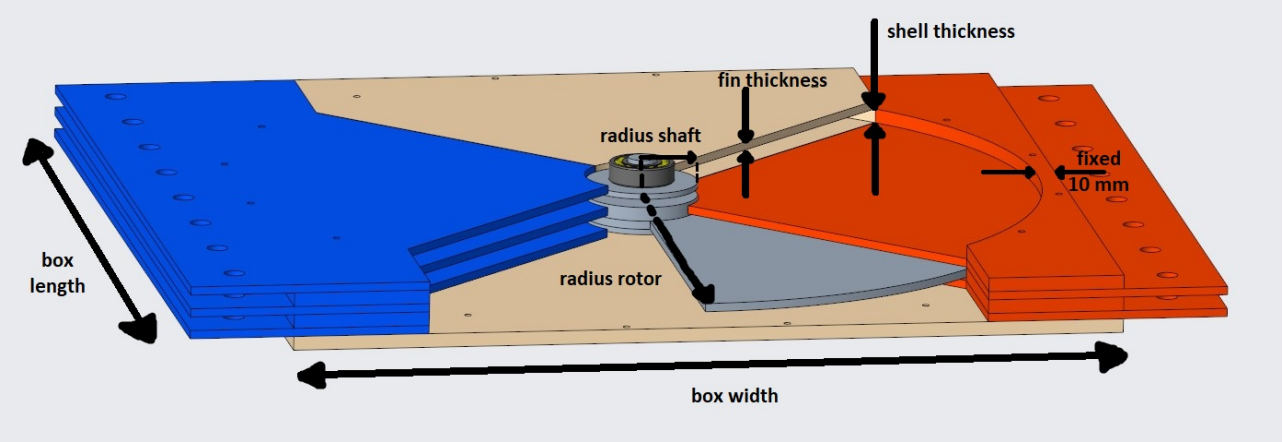

Figure 11: A schematic sectional view of how the dimensions are defined on the GREC.

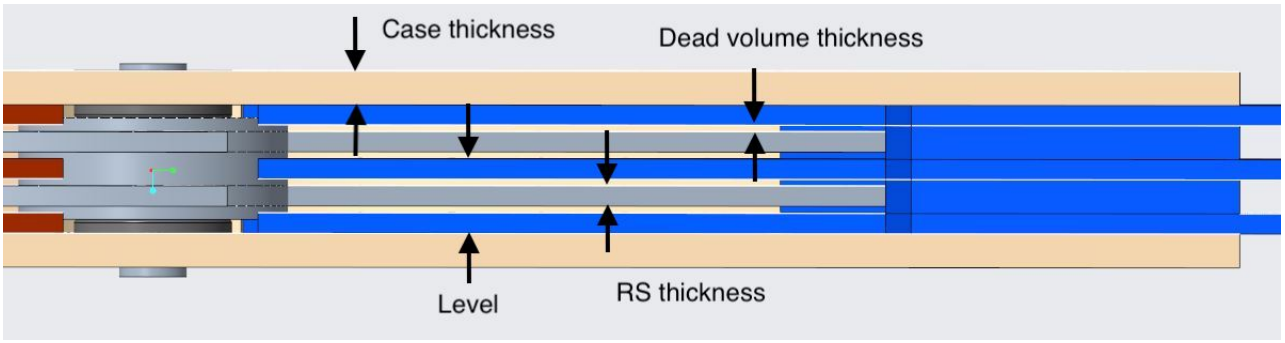

Figure 12: A schematic sectional view of how the dimensions are defined on the GREC. The definition of "Levels" is the number of rotation shutters that exist in the GREC-engine. One level also includes two conducting fins, one over the RS and one under.

The entire mathematical model-code is built based upon the standard input dimensions presented in table (1) and should be seen as the base scenario (scale 1). In order to obtain output results from larger models, a factor n is introduced. The factor i is a vector [1 2 3] and its purpose is to simulate three different sizes of the GREC. This will enable comparisons of different motor sizes in the results. In the code, the dimensions which carry a functional impact are added with the factor i. These dimensions are the length, width, radius rotor, radius shaft and level dimensions. The thickness of the RS, conducting fins and shell is not changed in this project because the ratio between them is crucial and has been established in advance.

3.1.1 Assumptions

To simplify the calculation model, the software MATLAB was utilized to construct the mathematical model. In the calculation model a number of assumptions were made and will be presented below:

- RS works frictionless.
- The work output was calculated as the work gained from volume change. The volume change in both compression and expansion are considered to be isothermal processes.
- The trait of the air in the GREC-engine is assumed to be an ideal gas and the parameters in table (2) were assumed at atmospheric pressure.
- All heat losses in the engine are neglected.
- The pressure after the isothermal expansion (p_2) is set to atmospheric pressure.
- The hot and cold source has an infinite temperature (the temperature doesn't vary when energy is received or rejected).
- The electric motor consumes 24 Watt for all rotation speeds and is scaled with the factor i.
- The WGV is in contact with the heat source for half the duration of a revolution (half the time it takes to complete one 360 degree rotation).

Table 2: The value of the air traits that was assumed at atmospheric pressure and 20 °C.

Symbol	Value	Unit
R	287	$\frac{J}{kgK}$
c_p	1005	$\frac{J}{kgK}$
k	0,0254	$\frac{W}{mK}$
ρ	1,189	$\frac{kg}{m^3}$
p_2	101325	Pa

3.1.2 Code structure

The size of the WGV is the body of the code, which was the first parameter that was calculated in the software. To calculate the volume, equation (8) and table (1) was used. Similarly the dead volume is calculated with its unique thickness and area. With the WGV and table (2) it was possible to compute the mass of the air in atmospheric pressure with equation (10), which later can be used to calculate the remaining pressures and volume change.

To get an overview of how the heat transfer coefficient (HTC) behaved in the model, the change of airflow needed to be computed along the radius. To calculate the radius of the WGV, equation (7) was used. The radius was later divided into ten segments of square pipes along the arc where an illustration can be found in figure (13). To compute the the hydraulic diameter (the characteristic length of a non-cylindrical pipe), the cross-section area and the circumference was needed. Because of an even distribution from the MATLAB-software, the cross section area and circumference was only calculated once with the equation (3) and (4). The hydraulic diameter was later calculated with the equation (11). Since the air velocity increased for each segment, it was computed with equation (5) in the middle of each segment (dashed lines). The reason behind this was to obtain a mean value of the velocity for the whole segment. Each value of the velocity for each segment was then put in a vector, where the first element in the vector was the segment closest to the centre. Thereafter a for loop was created so a HTC value could be established in each segment of the radius.

Table 3: The distance between the shaft of the GREC engine and the center of each segment (dashed lines), for the three different scaling. Segment 1 is the first dashed line from the centre.

Placement for each segment [m]										
Segment / Scaling	1	2	3	4	5	6	7	8	9	10
1	0.012	0.037	0.062	0.087	0.112	0.137	0.162	0.187	0.212	0.237
2	0.025	0.075	0.125	0.175	0.225	0.274	0.324	0.374	0.424	0.474
3	0.037	0.112	0.187	0.262	0.337	0.412	0.487	0.562	0.637	0.712

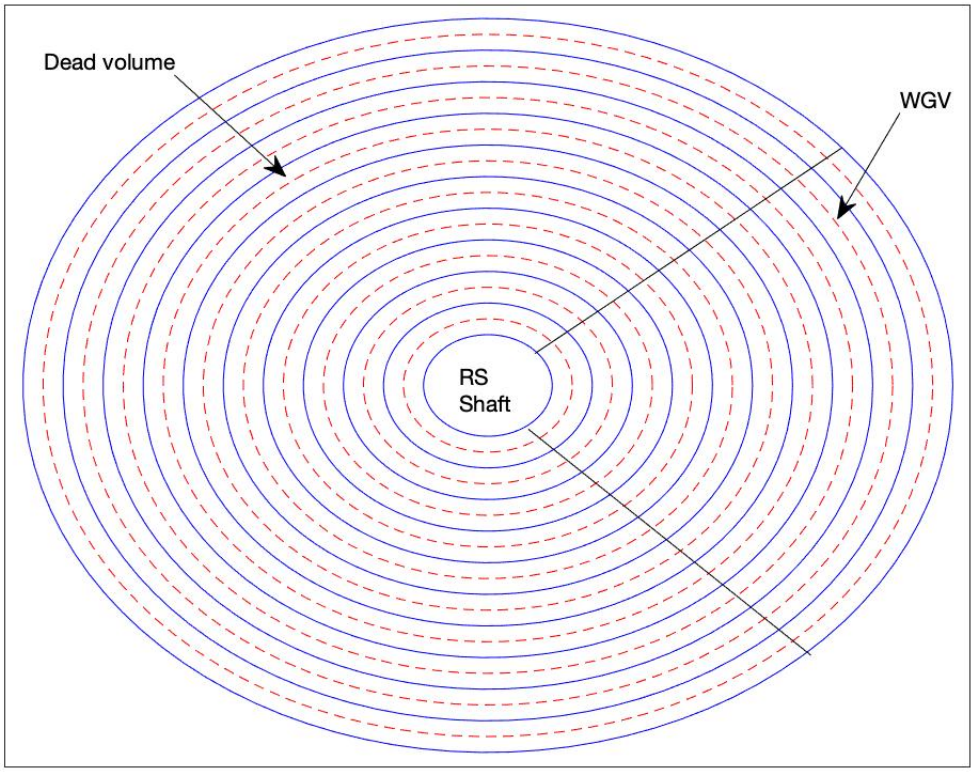

Figure 13: An illustration of how the segment was distributed along the radius of the RS. The solid lines represent the separation of each segment and the dashed lines is were the calculation for the tip speed and arc length was made for each segment.

To calculate the HTC in each segment, it was of high importance to establish if the airflow was laminar or turbulent in the segments. The following calculations were computed with help from the parameters in table (2). This was decided through the Reynold number which was calculated with equation (12). An "IF" command was then inserted in the code to see if Reynold number exceeded 2300 or not. The only thing left to decide before it was possible to calculate the HTC was to compile the Prandtl number of the air and Nusselt number. The Prandtl number was calculated with equation (13). To compute the Nusselt number, the arc length for each segment was needed. The arc length was computed with equation (2) and was inserted in equation (14) or (15) to calculate the Nusselt number dependent on the characteristic of the flow. With the Nusselt number it was possible to calculate the heat transfer coefficient with equation (16) in all of the segments.

By obtaining the HTC for the air in the dead volume and WGV, calculations of the transferred heat from the conducting fins could be extracted using Newtons law of convective heat transfer (17). This equation depends on the temperature of the WGV which also must be calculated simultaneously. To obtain a fair value of how hot and cold the volume alternately will become after a few revolutions, an iterative function simulating this is created. By calculating the heat transferred from the conducting fins, the amount of energy transferred to the WGV could be calculated by knowing the duration of which they are in contact. Utilizing the energy added and the first law of thermodynamics for a closed system, equation (18), a new temperature after the heating process could be retrieved. Obtaining the temperature after the cooling sequence is done by the same principal based on the new WGV temperature. This entire process is then repeated a sufficient amount of times until the temperatures reach an absolute value. A visual representation of the temperatures obtained from the iteration can be seen in figure (14). As a consequence of using these temperatures when calculating the input heat, the value obtained is an instantaneous power which in reality would change simultaneously as the actual WGV temperature changes. For the sake of time and simplification these instantaneous temperatures were however used in the calculations.

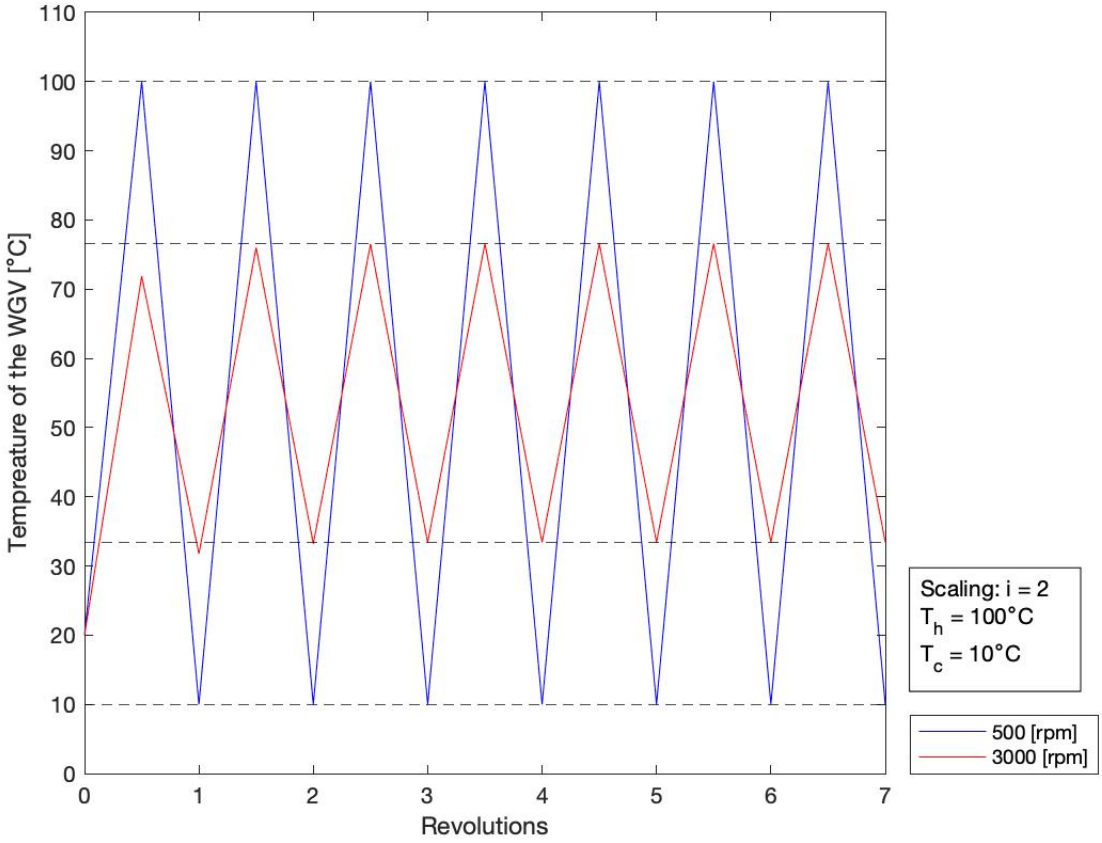

Figure 14: The alternating WGV temperature for two operation modes.

Assuming that the theoretical model operates according to the cycle visualized in figure (3), the operating temperatures are calculated according to the section above and p_2 is assumed to be atmospheric pressure, all remaining pressures and volumes can be calculated through the ideal gas law, equation (10).

The work that is done during both the expansion and compression can be calculated through equation (22), where the work for each process was calculated with equation (21). The expansion work is done between state 1-2 and the compression work is done through state 3-4, see figure (3). The net amount of work that effectively is extracted from the engine is the difference between the expansion and compression work. The power is then determined by multiplying the net work with the frequency of the rotation speed, equation (6). Having calculated the input heat and the net power output, the thermal and total efficiency of the motor can be calculated with equations (23) and (26), where $\dot{W}_{in}$ is the input power from the electric motor.

To understand how the GREC engine was affected by different parameters, a couple of tests were executed. The parameters that were considered to affect the engine the most was the rotation speed, source temperatures and model scaling. The first test that was executed was to see how the rotation speed affected the engine. For this test the temperature on the hot side was set to 100°C and the cold side to 10°C while the revolving speed change between 500, 1500 and 3000 rpm. The reason behind the interval was to get a clear picture on how the GREC's performance behaved while simultaneously retaining practically reasonable limits. This was done for three different scales, which is mentioned in chapter 3.1. The second test analyzed how the source temperatures changed the GREC's performance. The rotation speed was set to a constant value of 1500 rpm and the temperature on the heat source changed between 200, 350 and 500°C for all the three different scales of the engine. The same decision was made here concerning the choice of temperature intervals, however it was also important to keep in mind the maximum temperature the material theoretically could withstand.

3.2 Material analysis

With already existing drawings from nilsinside [14] the model was reconstructed in CREO Parametric 5.0. Each drawing was then made into a 3D part and thereon assembled with each other to match the corresponding physical model. This model of the GREC, see figure (15), would then be the source of all material simulations in ANSYS Workbench 2021 R1.

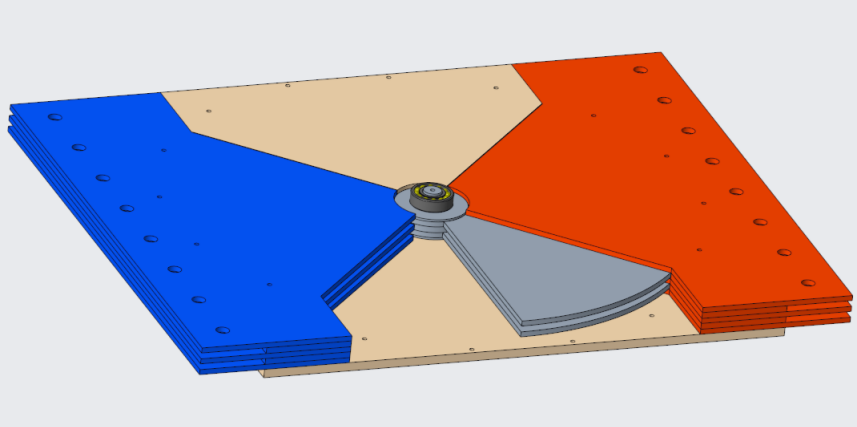

Figure 15: A completed assembled 3D model of the GREC with a cutout.

For the material analysis there had to be a mutual discussion with Nilsinside AB whether which parts should be considered as "crucial" in the GREC design. The discussion led into where the losses are located in the model. As described in section 2.4 there are heat, mechanical friction and fluid friction losses. The heat loss occur in the conducting fins and isolation module. The mechanical friction losses appear in the RS. With this in mind the choice became to examine the material of the larger parts which is the RS, the conducting fins, and the isolation material. Smaller parts such as bolts, bearings and the electrical motors shaft have not been a part of the material analysis.

3.2.1 Material selection

There are a number of things that have to be considered when deciding the material for the components in the GREC. To get an overview and a structure for which material that could be best suited for each crucial part, three different material analyses were made on the RS and the isolation material. Two different material analyses were made on the conducting fins. See table (4), (5) and (6) with material specifications taken from [13] and ANSYS material database Granta.

Table 4: Conducting fin material specifications and mean price in thousand SEK per cubic meter.

Material	k [W/mK]	c_p [kJ/kgK]	ρ [kg/m^3]	Price [TSEK/m^3]
Aluminum alloy	194	0.90	2700	49
Copper alloy	394	0.38	8942	479

Table 5: Isolation material specifications and mean price in thousand SEK per cubic meter.

Material	k [W/mK]	c_p [kJ/kgK]	ρ [kg/m^3]	Price [TSEK/m^3]
Steel	56.6	0.448	7850	56.2
Bakelite	0.141	1.47	1243	28.2

Table 6: Revolving shutter material specifications including yield strength and mean price in thousand SEK per cubic meter.

Material	k [W/mK]	c_p [kJ/kgK]	ρ [kg/m^3]	Yield Strength [MPa]	Price [TSEK/m^3]
Polystyrene	0.12	1.2	1070	50	11.2
Magnesium alloy	25	1	1830	193	54.7
ABS 10% carbon fiber	0.36	1.64	1040	74	49.6

The material quality to be heat resistant should be applied to the isolating module since these parts should keep the thermal energy inside the gaseous volume. These material qualities are described by the heat capacity, c_p and heat-transfer rate, k. As a pair these values should be low for the insulating materials. therefore a material with said qualities should be chosen here.

The conducting fins must conduct and emit heat at a high rate to the WGV to get great temperature- and pressure differences. This requires the opposite material qualities compared to the isolating module. The conducting fins need to have a high heat capacity and high heat-transfer rate to be able to absorb the heat from either the hot or cold heat storage while emitting this heat to the WGV.

To make the revolving shutter move more easily the weight must be reduced by constructing the RS from a light yet thermal resistant material as mentioned earlier. To get a low mass for the revolving shutter a low density, ρ should be searched for when determining the material. If the RS is lighter, the electric motor input can be lowered and the overall efficiency will be increased. For example with the ABS carbon fiber material in table (6). This is a thermoplastic with low density and decent heat resistance, which would be a good option for the RS.

3.2.2 Simulation guide

To simulate the RS, both rotational force and thermal load were implemented on to the revolving shutter. This was implemented to simulate the centrifugal force and the thermal difference established through out the GREC. These two conditions will result in a stress developing in the RS which in turn will create a deformation on the RS. The larger rotational force and higher temperature, the larger the deformation will be. The thermal load coming out of respective heat storage will also give temperature plots in the conducting fins and isolation module to distinguish where the heat is transferred.

The operating conditions implemented on the GREC ANSYS model is:

- Temperatures for the hot (T_h, red side) and cold (T_c, blue side) storage assigned on respective sides of the conducting fins along the side named "box length" visualized in figure (1). The temperatures are 100°C and 10°C.
- The average temperature result of the RS is set to the entire RS. Since ANSYS only simulates the rotation and does not affect actual movement. This implies that if the average temperature would not have been applied, the RS would instead have a cold and a hot side.
- A rotational velocity set to 90 rpm for the revolving shutter and standard gravity for the whole model.
- "Displacements" set to zero on every part but the RS locking the rest of the GREC-model in place.
- Material assignments of the materials in table (4), (5) and (6) to the corresponding parts one material to each part at a time.

3.3 GREC construction improvements

For analyzing and to be able to pinpoint GREC construction improvements the use of a scaled quality approach were utilized using Six Sigma[15]. Without mentioning Six Sigma too much since this quality approach is rather heavy, our approach will therefor be a scaled Six Sigma approach that will more define future quality improvements and an easier operating usage. The scaled Six sigma model and its three tools are as follows:

1. **Define**
   Identification of the problem and defining whether the problem for GREC in this stage of its TRL value should be considered or not, depending on the purpose for quality improvements and operating usage.
2. **Measure and analyze**
   Determine the cycle capability with measured data which will be analyzed throughout the GREC cycle and with this understand the reasons for the cause of the identified problem. In this tool the exploration phase is covered, which is important because most of the understanding for the problem between the process variables and the development of theoretical improvements are gained.
3. **Improve**
   With the help of the tools above there should now be an identified root cause and broader understanding of available improvements that could be implemented on the GREC. In this tool the clarification and a pinpointed construction improvement is then determined as a path for a solution for the problem.

4 Results

In the following chapter the result from the mathematical model in MATLAB, the simulation in ANSYS and construction improvements of the physical model will be presented.

4.1 Mathematical model system

The following result will represent the outcome from the mathematical model in MATLAB. This section is divided in three subsection where all results in these sections compare three different scalings of the GREC engine. The first section contains the result on how the HTC changes along the radius, the second contains result on how different the engine speed affects the GREC engine. The third and the last section contains the result on how thermal and the total efficiency changes when the interval between hot and cold temperature changes.

4.1.1 HTC along the radius of the conducting fin

In this subsection the results of the Reynolds number and HTC will be presented for both WGV and the dead volume. This will give an overview where the transit between laminar and turbulent flow befall and how it affects the HTC value. The revolution speed used for the coming result was 1500 rpm, however studies for 500 rpm and 3000 rpm were also made which is presented in chapter 8.

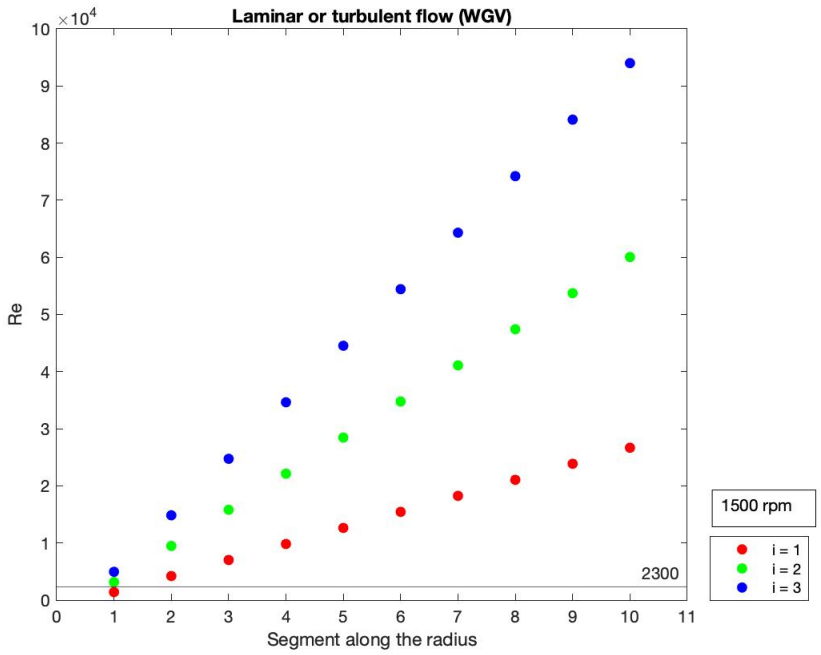

Figure 16: A panoramic view on how the Reynolds number changes along the segments in the WGV. The colours represent different scaling of the GREC engine, where the red dots represent the original scaling, the green 2 and the blue 3. The black horizontal line is appointed at 2300 and is meant to represent the transit between laminar and turbulent flow.

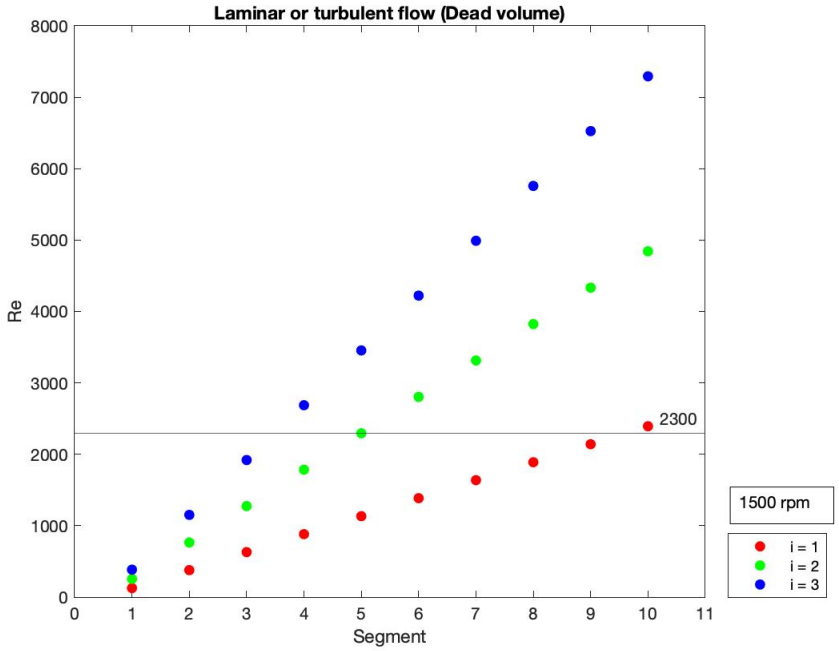

Figure 17: A panoramic view on how the Reynolds number changes along the segments in the dead volume. The colours represent different scaling of the GREC engine, where the red dots represent the original scaling, the green 2 and the blue 3. The black horizontal line is appointed at 2300 and is meant to represent the transit between laminar and turbulent flow.

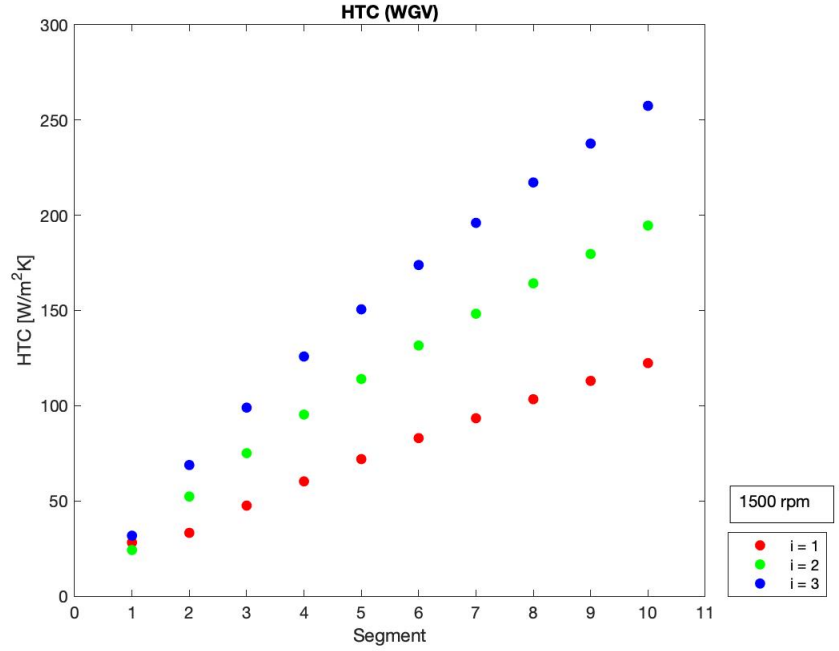

Figure 18: A panoramic view on how the heat transfer coefficient (HTC) changes along the segments in the WGV. The colours represent different scaling of the GREC engine, where the red dots represent the original scaling, the green 2 and the blue 3.

Table 7: The specific value of HTC for each segment in the WGV, which are shown in figure (18).

HTC $[W/m^2K]$										
Segment / Scaling	1	2	3	4	5	6	7	8	9	10
1	28.2	33.2	47.5	60.2	72.0	83.0	93.4	103.4	113.0	122.4
2	24.2	52.3	75.1	95.3	114.0	131.6	148.3	164.3	179.7	194.6
3	31.7	68.8	99.0	125.8	150.6	173.9	196.0	217.2	237.7	257.5

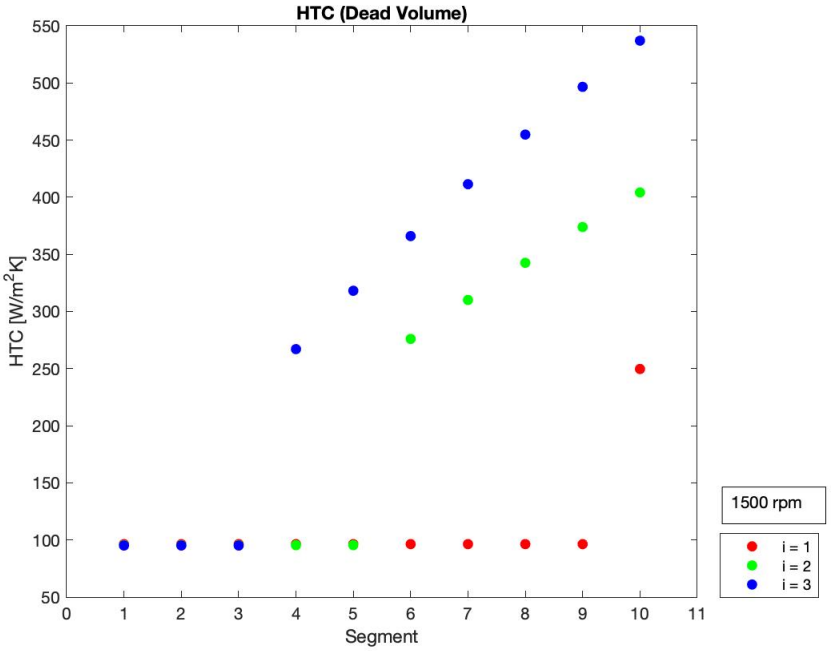

Figure 19: A panoramic view on how the heat transfer coefficient (HTC) changes along the segments in the dead volume. The colours represent different scaling of the GREC engine, where the red dots represent the original scaling, the green 2 and the blue 3.

Table 8: The specific value of HTC for each segment in the dead volume, which are shown in figure (19).

HTC $[\mathrm{W/m^2}K]$										
Segment / Scaling	1	2	3	4	5	6	7	8	9	10
1	96.4	96.4	96.4	96.4	96.4	96.4	96.4	96.4	96.4	249.7
2	95.5	95.5	95.5	95.5	95.5	276.0	310.0	342.6	373.9	404.2
3	95.2	95.2	95.2	267.1	318.1	366.0	411.4	454.8	496.6	537.1

4.1.2 Output data with different rotation speeds

In this sub-chapter relevant output parameters for different rotation speeds are displayed. Hot and cold source temperatures are constant at T_h=100°C and T_c=10°C respectively.

Table 9: The mean value of the HTC in the WGV for different rotation speeds and model scales.

HTC [W/m^2K]			
Scaling / [rpm]	1	2	3
500	35.7	54.7	71.5
1500	75.6	117.9	155.8
3000	121.8	193.7	256.4

Table 10: The mean value of the HTC in the dead volume for different rotation speeds and model scales.

HTC [W/m^2K]			
Scaling / [rpm]	1	2	3
500	95.2	94.3	109.5
1500	111.7	218.4	313.7
3000	220.0	394.4	532.3

Table 11: Net power output as a function of rotation speed and scale.

Power output [W]			
Scaling / [rpm]	1	2	3
500	24	452	1 528
1500	38	728	4 585
3000	53	952	6 023

Table 12: Input heat as a function of rotation speed and scale.

Heat input [W]			
Scaling / [rpm]	1	2	3
500	323	4 630	15 645
1500	586	9 057	46 936
3000	885	13 327	70 542

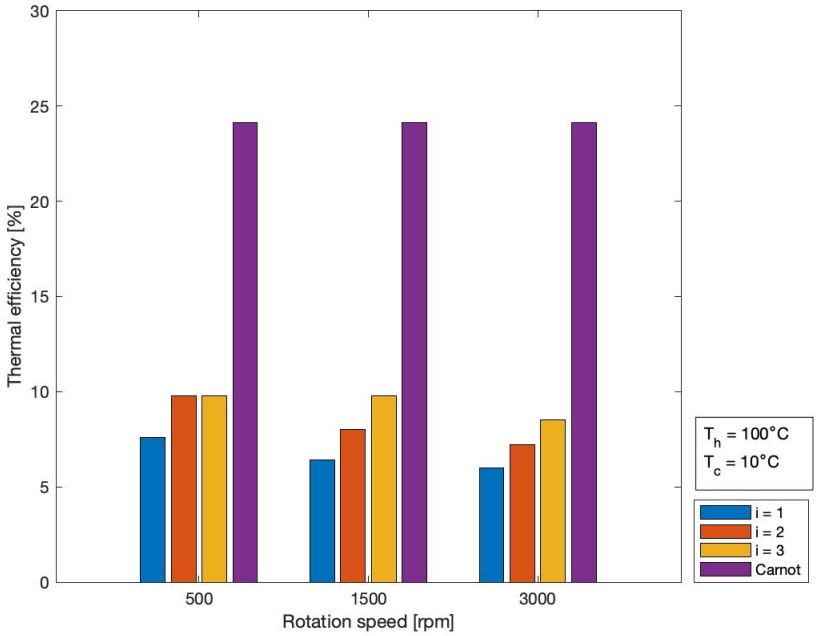

Figure 20: Thermal efficiency as a function of rotation speed and the scale of the GREC engine, where the blue, red and yellow staples represent the the different scaling and the purple staple represent the theoretical Carnot efficiency. The specific value for each bar can be found in table (17) and (18) in Chapter 8.

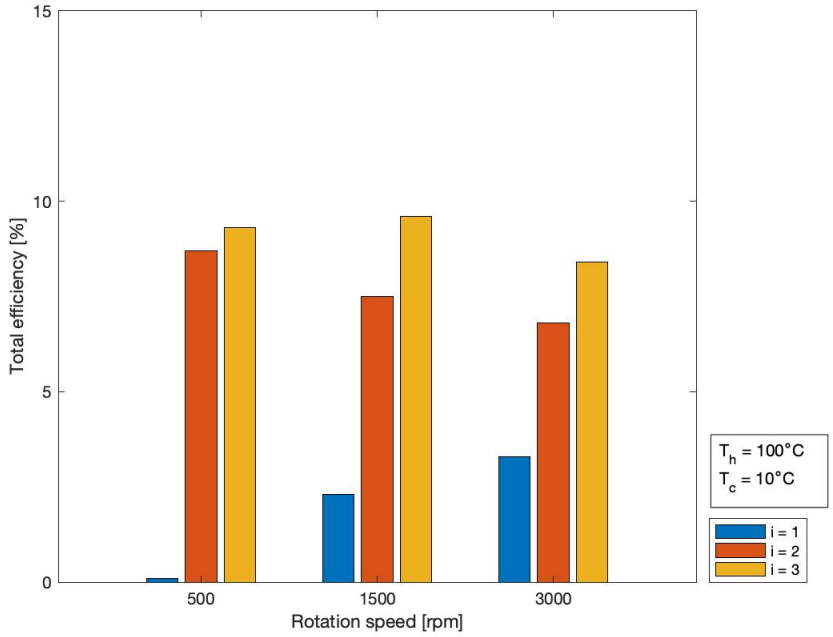

Figure 21: Total efficiency as a function of rotation speed and the scale of the GREC engine. The specific value for each bar can be found in table (19) in chapter 8.

4.1.3 Output data with constant rotation speed and temperature changes of the heat source

In this sub-chapter the theoretical model efficiency is displayed for higher temperatures of the heat source, with a constant sink temperature of T_c=10°C and constant rotation speed of 1500 rpm.

Table 13: How the Power output changes with an increase of temperature on the heat source.

Power output [W]			
Scaling / T_h [°C]	1	2	3
200	169	3 145	19 206
350	498	9 065	54 137
500	950	17 029	100 340

Table 14: How the Heat input changes with an increase of temperature on the heat source.

Heat input [W]			
Scaling / T_h [°C]	1	2	3
200	1238	19 120	99 087
350	2210	34 210	177 310
500	3190	49 310	255 540

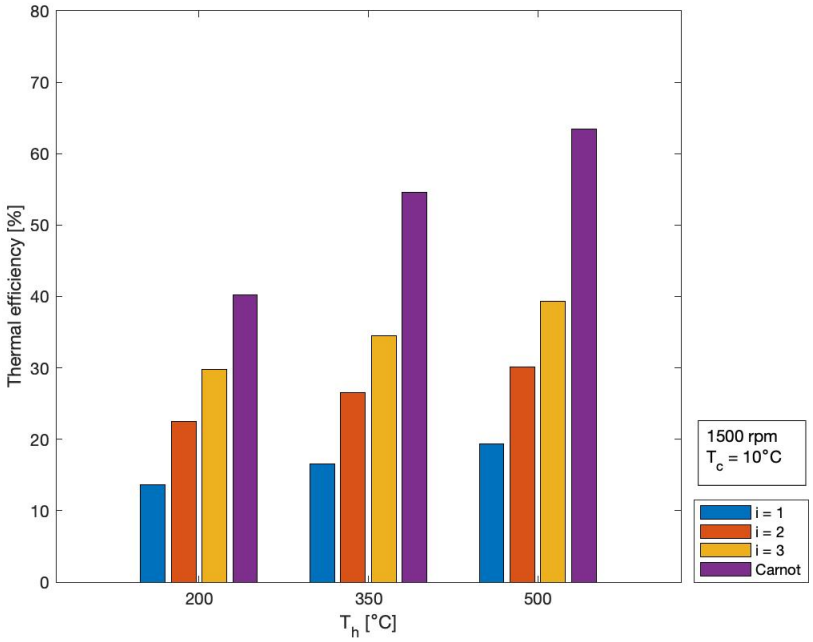

Figure 22: Total efficiency as a function of rotation speed and the scale of the GREC engine. The specific value for each bar can be found in table (17) and (20) in chapter 8.

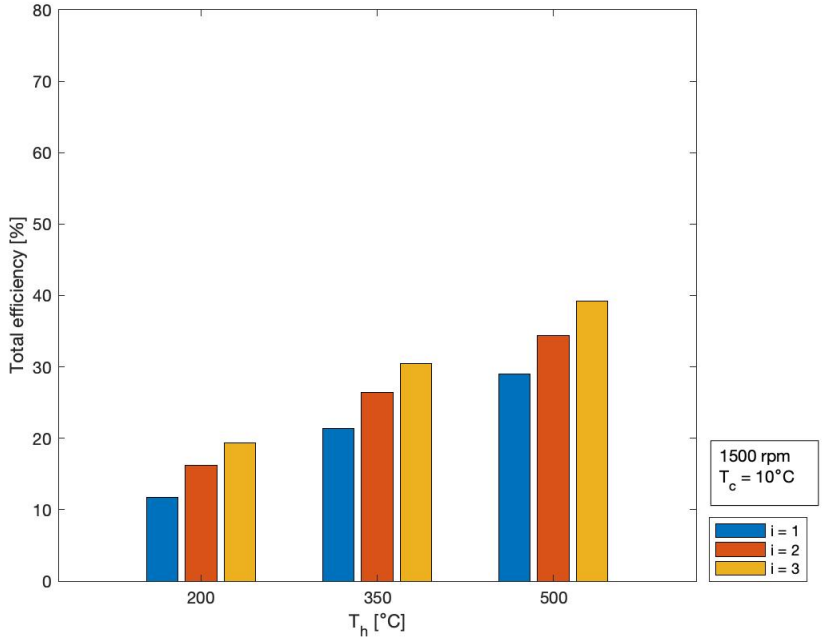

Figure 23: Total efficiency as a function of rotation speed and the scale of the GREC engine. The specific value for each bar can be found in table (21) in chapter 8.

4.2 Material analysis

The results from simulating in ANSYS, as mentioned in section 3.2.2, will be presented with coloured plots and numeric values for the different materials and parts.

4.2.1 Conducting fin and isolation material

Material analysis and results for the conducting fins and isolation module was made with the materials in table (4) and (5). These materials create four different combinations and are presented in figure (24) and (25) with aluminum as the conducting fin material with steel and bakelite isolation. Results for the copper alloy conducting fin can be seen in the appendix and in figure (36) and (37).
The isolating module set in between the two conducting fins. They can be discerned by the four thin black lines which connect to the center hole. In figure (25) the isolating module is easily distinguished. The red area indicates a high temperature and the blue indicates low temperature.

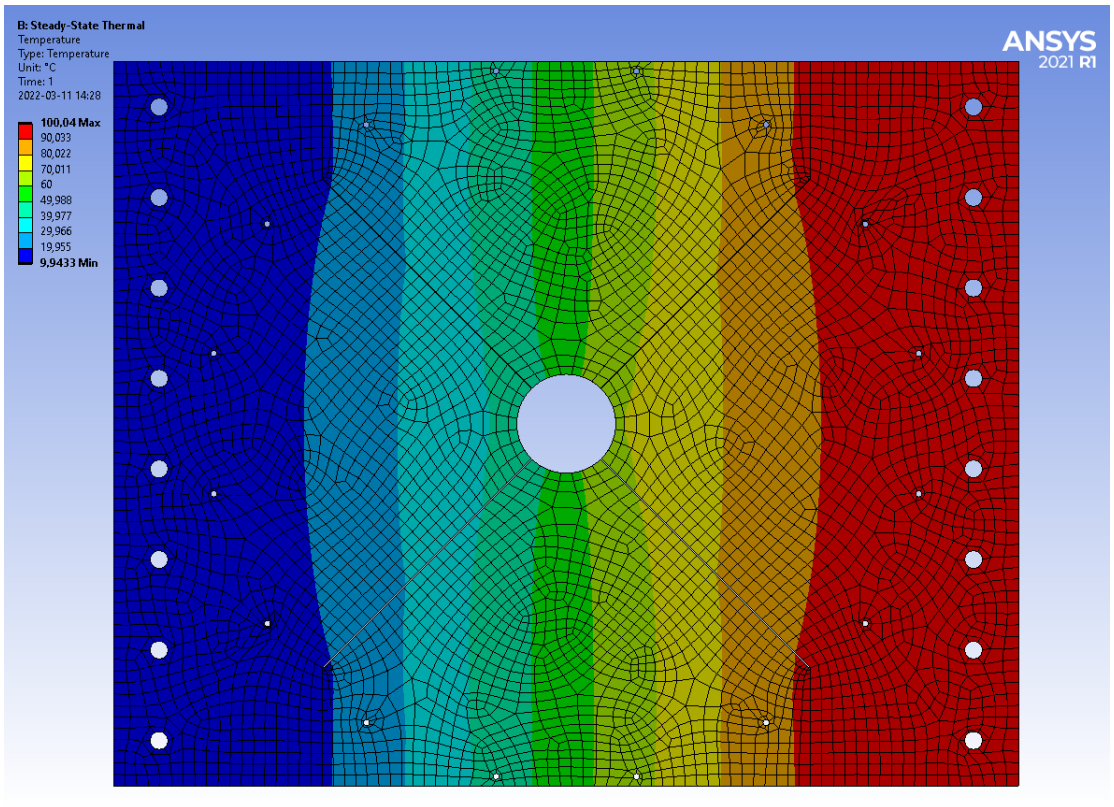

Figure 24: Temperature plot of the aluminum conducting fin and isolating steel.

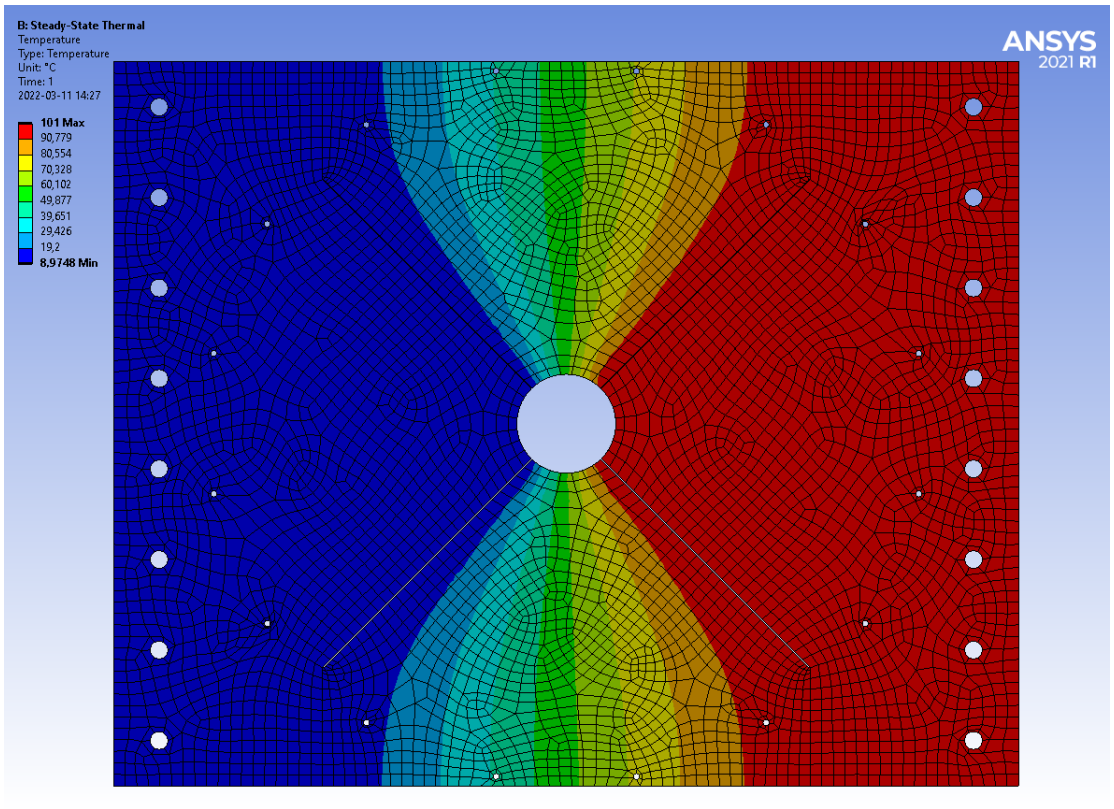

Figure 25: Temperature plot of the aluminum conducting fin and isolating bakelite.

4.2.2 Revolving shutter material

The revolving shutter materials from table (6) were used to simulate operating conditions. From the simulation, plots for the deformation and stress could be created as in figure (26) for polystyrene. All the other revolving shutter materials resulted in the same pattern of deformation and stress however not the same values. The corresponding deformation and stress value for each material is presented in table (15). Stress and deformation plots of ABS thermoplastic and magnesium alloy can be found in the appendix in figure (38) and (39). In these figures the red area indicates the highest stress or deformation while the blue area indicates the least.

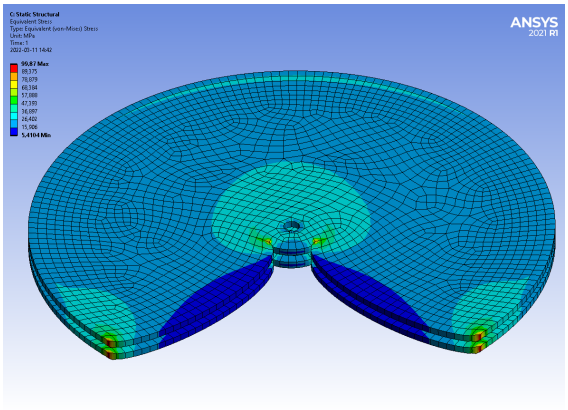

(a) Stress plot for the revolving shutter using polystyrene.

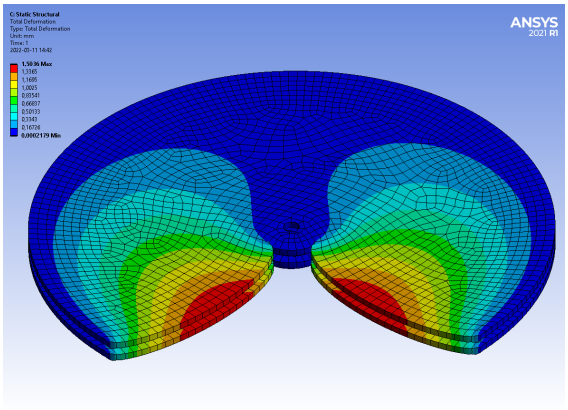

(b) Deformation plot for the revolving shutter using polystyrene.

Figure 26: Resulting deformation and stress plots from ANSYS for the revolving shutter using polystyrene.

Table 15: Resulting deformation and stress values for the revolving shutter.

	Stress [MPa]		Deformation [mm]	
Material	Maximum	Average	Maximum	Average
Polystyrene	99	25	1.5	0.35
Magnesium alloy	346	82	0.34	0.079
ABS 10% carbon fiber	56	14	0.37	0.086

4.3 GREC construction improvements

To understand our improvement results there is a need for visualisation of the GREC physical model as presented in figure (27). The results are presented in order of most important to least important. The problem is first stated as defined, second the measure and analyzing and last the improvement were pinpointed.

Table 16: List of improvements using Six Sigma.

Define	**Measure and analyzing**	**Improvement**
Malfunctioning GREC.	Cycle data show friction inside GREC and can be clarified with the noise the rotor is making when operating, root cause is wrong assembled fins that create a non frictionsless surface.	Reassemble fins.
Temperature sensors misguiding.	Operating data show different room temperatures even when GREC is not operating. When in operating mode the same problem still exists. Root cause is either broken sensors, wrong code or wrong assembled sensors.	Open up GREC and do an ocular inspection, look over the code and as last resort switch all sensors to new ones.
Leakage of pressure.	While in operating mode the electric motor moves because of the force it is creating from the movement of the rotor. This creates cracks in the tightening around the electric motor, which lead to leakages.	Find a better solution for the assemble of the electric motor.
No cold reservoir.	In the bottom in figure (27a) where there are lots of lights there is a sort of reservoir fins. The fins will enable the heat transfer on that side of the GREC. This problem leads to the conclusion that this model can only change reservoir temperature on one side.	Assemble a possible cold reservoir.
Control interface incoherent.	By iteration this problem becomes clear. By changing speed, delay and even when the start and stop functions are implemented, the interface sort of shuffles and becomes incoherent. This leads to difficulties for the user usage. Root cause of the problem are the existing code.	Troubleshoot the existing code.
Overview of all cabling.	Referring to figure (27) the cabling is messy and create difficulties when troubleshooting. The circuit board is assembled by tape which has started to loosen. This has created problems due to loosened cables which affected data gathering.	Make a new circuit board with a better overview, having longer cables with markings and also improve the soldering. Take away the circuit board from the physical model and place it in a box.

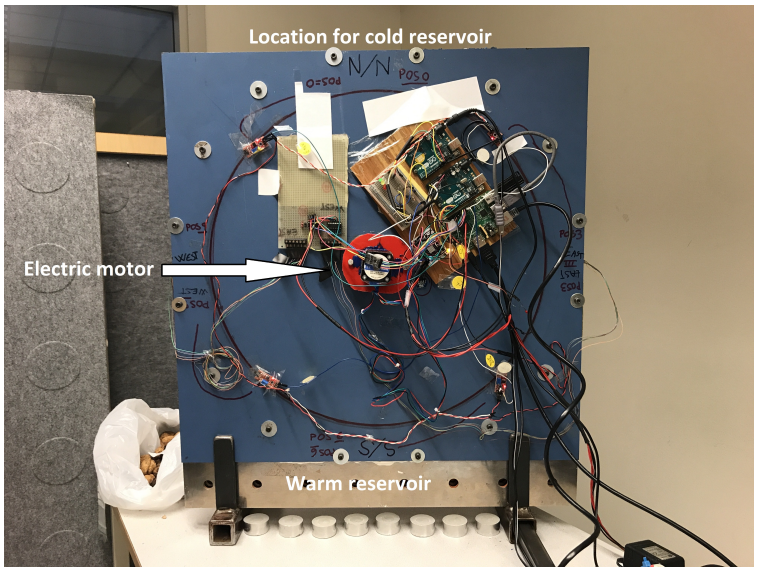

(a) Overview of physical model.

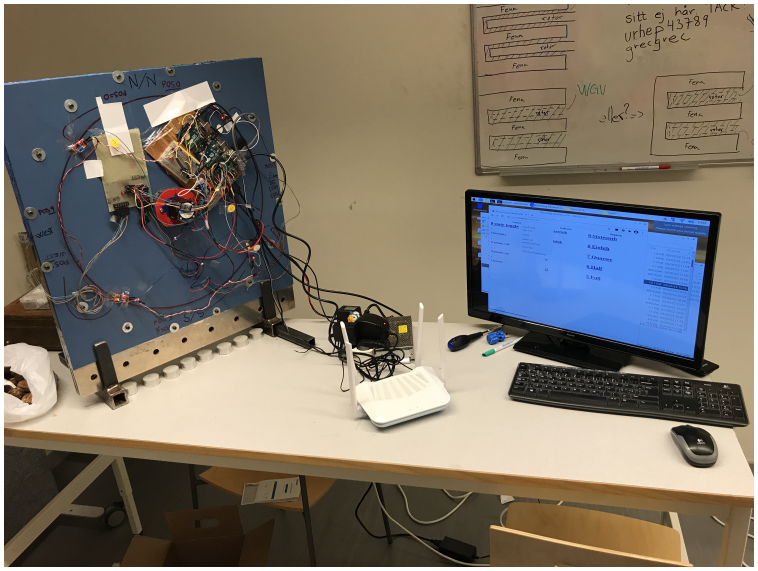

(b) Overview of physical models working space.

Figure 27: An overview of the GREC, physical model and its surrounding working space.

5 Discussion

The following discussion is separated into three categories, mathematical models, material analysis and GREC improvements.

5.1 Mathematical models

According to figures (16)-(19) and tables (7)-(8) it can be observed that the Reynolds number and HTC increase for each segment along the radius. This outcome was expected since both parameters depend on the velocity of the air which also should increase further away from the center of rotation (linearly with the RS).

Reviewing the results of the Reynolds number and the HTC for the segments of air volume it can be noted that the Reynolds number becomes close to 10 times larger in the WGV than in the dead volume for 1500 rpm, compare figure (16) and (17). Meanwhile the HTC becomes nearly 2 times smaller in the WGV compared to the dead volume, see figure (18) and (19). Considering the fact that a higher Reynolds number generally yields a more turbulent airflow, the air in the WGV should be significantly more turbulent than in the dead volume according to the result. A larger Reynolds number also yields a larger Nusselt number which in turn should magnify the HTC according to equation (16). The hydraulic diameter (d_h) which is larger in the WGV does however limit the magnification of the HTC relative to the dead volume with a smaller d_h, hence delivering a larger HTC in the dead volume. By observing table (9) and (10) which represents the mean value HTC for three rotation speeds and scales, this becomes very apparent. Since a large HTC in the dead volume is unwanted for the performance of the GREC, the proportions of thickness for the dead volume should be reconsidered to be larger to prevent a large HTC.

Tables (11) and (12) displays the net power output and the input heat added to the WGV respectively. Increasing the rotation speed marginally increases the output power at a slower rate than the input heat, clearly displayed in figure (20). Generally by increasing the rotation speed it would be expected to see better performance, but in this case a larger rotation speed limits how large the generated work becomes. This can be explained by observing figure (14) in chapter 3.1.2. If the motor runs too fast the WGV won't be able to reach the maximum temperatures which the sources allow even though the maximum amount of input heat is supplied. If the temperature differences become smaller, so does the generated work. So if the rotation speed is too high, a negative trend in thermal efficiency is induced.

Larger improvements appear when the model scale is enlarged. A larger model has a higher capacity in volume, available convective heat transfer area and air velocity (tip speed), resulting in a positive efficiency growth. A higher air velocity and area of convection entails that the heat transfer rate becomes larger, therefore allowing more energy to be transferred and larger temperature differences of the WGV for every revolution. As long as the heat rate and rotation speed doesn't allow the temperature to exceed the temperature of the sources (which is practically impossible), efficiency will increase to a certain point which hasn't been established in this report. One apparent case where this happens is in figure (20) for scale 2 and 3 at 500 rpm. In these operating modes the heat rate relative to the rotation speed is so fast that more energy than what is required to increase the temperature to the max temperature T_h, is available. The input heat and output power is therefore limited since maximum temperature differences are produced for every revolution. The behaviour of the total efficiency in figure (21) is similar to the thermal efficiency except in scale 1 with 500 rpm where the power of the electric motor almost is as large as the thermal net work output, resulting in a poor efficiency. In figure (22) - (23) where different temperatures on the heat source are analyzed, it shows that higher temperature differences increase efficiency, predictable according to Carnot, equation (25). Increasing the temperature from 100°C to 500°C also increases the power output from 4 585 W to 100 340 W for scale 3 at 1500 rpm, compare table (11) and (13). The heat input does consequently increase as well but significantly less than the power output, therefore improving the efficiency. The efficiency never exceeds the theoretical Carnot efficiency which is good and enforces the applied method used.

Generally the method used to create the mathematical model is considered accurate relative to the assumptions and simplifications applied. But in order to completely verify the reliability of the mathematical model, real experiments with similar operating modes must be conducted and compared. Most of the assumptions applied are regarded to be necessary to obtain the sought out parameters with a few exceptions. Losses in the GREC are completely neglected in the calculations where they actually could be implemented by either an effort to calculate them or to make reasonable assumptions. The heat sources were set to an infinite temperature and therefore no regards were made for how much heat they required from an external source. This could however have been computed as well to obtain an estimate of how well the heat would spread in the fin and how much supplied heat the fins would require to maintain the set temperature. However, this would consume much valuable time and was therefore not in the scope of this project.

5.2 Material analysis

The results of the analysis for the conducting fins and isolation materials featured in figure (24) and (25) show the heat distribution. Comparing the difference of steel in figure (24) and bakelite in figure (25) for isolation material there is a clear change of where the heat is conducted. With steel as isolation the heat is spread across the conducting fins and isolation. About half of the conducting fin area does not reach maximum temperature. Meanwhile for the bakelite, heat is barely conducted to the isolation material. This translates to more spread of heat distribution in the conducting fin. A higher temperature all across the conducting fin leads to more heat transferred to the WGV and will contribute to more power output for the GREC. therefore the isolation material should be bakelite and not steel.

Comparing the conducting fin material aluminium in figure (24) and (25) to copper in figure (36) and (37) the results have more resemblance. There is a slightly higher distribution with copper that comes from the higher heat-transfer rate, k in table (4) for copper. The considerably faster heat-transfer for copper also signifies that the heat conducted to the WGV from the conducting fin can be replaced more promptly. This implies that the conducting fin temperature can stay more or less constant whilst heat is conducted to the WGV. Which means more heat will be transferred to create higher pressure differences and increase work output.

The revolving shutter was tested with three different materials. All three received different results in stress and deformation presented in table (15). ABS plastic had the lowest stress at 56 MPa seen in figure (38a). This was expected since it is the most heat resistant of the three materials. Polystyrene is exposed to 99 MPa and in last place we find the Magnesium alloy at 346 MPa visualized in figure (39a). The yield strength for the different materials in table (6) shows that both Polystyrene and the Magnesium alloy will both exceed their yield limit of 50 MPa respectively 193 MPa. This results in both polystyrene and magnesium alloy achieving permanent plastic deformation. But as presented in figure (26a), there is just a very small part of the RS that gets exposed to the maximum stress. Only this area will receive plastic deformation. And these two revolving shutters can not be used with the current RS structure.

A main portion of the stress established, originated from the heat transferred to the RS. This came to our attention when significantly raising the rotational velocity and the stress barely increased. This is why the magnesium alloy RS resulted in much greater average stress due to the higher heat-transfer rate, k listed in table (6). The ANSYS simulations might therefore be slightly inaccurate and misleading since this came to us as a surprise and no further analyzes have been made regarding this. If this supposition is wrong and the rotation velocity does affect the stress. The hot side temperature could be lowered and the two other revolving shutters could be used without reaching their yield limit.

The air space between the RS and the conducting fin is slim. From table (1), the distance is 0,5 mm on either side of the RS. Mechanical friction is established here by the RS rotating against the conducting fin. Deformation on the revolving shutter might then lead to an increase in friction. In table (15) all the deformations are relatively small and do not affect the friction more or less, except for the deformation in the polystyrene. A deformation of 1,5 mm on the RS occurs when using polystyrene. This might interfere

with the rotation of the RS. Although in figure (26b) the deformation is concentrated to the 1/4 opening on the RS. If this deformation is in the direction of the thickness on the RS it will make the rotation heavy and get hindered by the deformed RS. Another aspect that will make the rotation heavy is the weight of the RS. The weight is determined by the density, ρ in table (6). The lightest material is ABS thermoplastic with a density of 1040 kg/m^3. The polystyrene is just a bit heavier, and the magnesium alloy is almost twice the weight. This means the ABS will be, in relation to the other materials, much easier to rotate. Hence less power is needed from the electrical motor for the same amount of movement.

In conclusion the stress in the revolving shutter causes permanent deformation for polystyrene and magnesium alloy in small areas. Hence these materials can not be used with the current shape of the RS or these high temperatures. The low density of ABS is mitigating for the power needed. The best material would be the ABS thermoplastic with its high yield strength and low heat-transfer rate.

The price varies quite a bit when it comes to the different materials of the GREC. For the conducting fin, copper and aluminum has been tested. The price is almost ten times higher per m^3 for copper compared to the aluminum, shown in table (4). As mentioned earlier the copper has better heat transfer qualities. This leaves the question whether it would be worth upgrading the aluminum fins to copper fins. Bakelite is the clear choice for the isolation material. It is cheap and has low heat transfer qualities meaning it isolates well. It is cheaper than steel, making it better in every aspect. If price was the only aspect taken into consideration when choosing the material for the RS, polystyrene would by far be the clear choice. Polystyrene is also heat resistant which is preferable but it has low yield strength that might cause it to break.

5.3 GREC improvements

As presented in table (16) the results indicate that construction improvements could be made. With the knowledge of utilizing the scaled Six Sigma approach some defined problems are more important than others. For example the three first problems, malfunction GREC, temperature sensors misguiding and leakage of pressure is highly recommended to solve. These problems have the highest impact on the GREC as presented in the measure and analyzing section in the table (16). The malfunction problem is rather in need of solving to even get the physical model operating cycle to be working at all. Since the root cause states that the problem is a wrong assembled fin causing friction, the only choice in this situation is to open up the GREC and start from the beginning of the assemble and redo the work. Friction is something that can not be avoided and will always be present during a heat engine operating cycle [16]. The importance of reducing friction is high since it causes a negative loss in efficiency. In this case the work output W is going to be reduced to zero because the friction of the fins is causing malfunction.

The problem regarding the misguiding sensors is also important due to that it is a main data analyzing point. The data from the sensors can be used to analyze the heat transfers inside GREC. The sensors are the only source that will provide suitable information regarding the temperature change of the GREC cycle. To improve the sensors it might be necessary to open up the GREC if the programming code does not provide a solution. By opening up the GREC the recommendation is to solve both the malfunction and temperature sensor's problems since it is rather cumbersome to reassemble the GREC.
This leads into the last of the three main defined problems, the leakages of pressure, whose root cause is depending on how well the tightening has been done. With the approach of Six Sigma the main pressure leakages came from the area around the assembled electric motor. What this leakage will do is to affect the pressure change which the GREC is trying to create, therefore leakage will decrease the efficiency. The solution for this is to provide a new assemble style of the electric motor, since the current assembly solution can not provide a good enough tightening.

The defined problem "No cold reservoir" became more important than we thought from the beginning because of the temperature balance it is creating regarding the heat transfers inside GREC. As referred in measure and analyzing in table (16) the conclusion is that only one side of the GREC is able to create heat. Then when the GREC is in operating mode and in the phase when the heated WGV, from the hot-tempered

reservoir, is entering the non existing cold-tempered reservoir the heat transfer is minimal or even none existing. Then in the long run each cycle will instead of the ground principle of lowering the temperature of WGV heat it up instead. So with each cycle the supposed cold-tempered reservoir is going to become warmer and warmer and with each cycle the temperature of the WGV will have less change. With this in mind the efficiency will become lower the higher temperature the cold-tempered reservoir becomes. With equation (25) the visualisation can be provided, due to less change between the two temperatures T_H and T_L, the η_{th} will decrease. This leads to the technology that the GREC should be providing when creating two temperature reservoirs and with that a possible pressure change during the GREC cycle will fail. This could even be cross-referenced to the reversible isothermal compression in the Carnot cycle in figure (6), without an energy sink that will provide a cold-tempered reservoir there will not be any compression. This leads to the piston not moving and the heat engine will not be able to provide work. therefore the assembly of a cold-tempered reservoir should be done either in this physical model or in future upcoming models to further extend the quality of GREC.

The remaining two problems are the less important ones, but nevertheless need to be solved since it has caused problems regarding operating usage, troubleshooting and data collection. The last two improvements that are listed in table (16) are more time consuming work since it is more of a methodical procedure. By solving this the user experience, data analyzing and even the troubleshooting processes will become much easier. This will lead to an increased professional appearance of the GREC.

Summarized, the improvements that are pinpointed should be considered as a path to better results and functionality for the GREC. Since all defined problems do not provide a full solution, for example "a better solution for the assemble of the electric motor", the scaled quality approach using Six Sigma can only deliver the root cause but not a full solution. But just because there is not a full solution to the defined problem, the procedure is measured and analyzed. Further on the pinpointed construction improvements could then be listed as a path to future work and thereby raising the current TRL value and provide a guide forward for future work.

---

6 Conclusion

A mathematical tool for performance calculations has been developed during this project to theoretically verify the technology of the GREC. By applying a few simplifications and assumptions, the tool provides reasonable results compared to scientific theory. How different scales affect the performance of the GREC was examined and results showed that a larger GREC model would be more effective and able to produce more power at several given source temperatures. The rotation speed proves to impact the heat transfer capability in the engine, primarily by affecting the magnitude of the heat transfer coefficient but also the achieved temperature difference in the WGV. A higher temperature difference between the heat sources also leads to a significantly higher obtained power output and efficiency, making it a promising concept to study further.

Three different materials are needed for the three parts of the GREC. The conducting fins(conducting fin) need good heat transfer and the best material would then be the copper alloy. Considering the high price of copper, the other material aluminum is still very good and is a great choice for a low price. For the isolation, there is no question that bakelite will increase the performance since the heat is better distributed in the conducting fin whilst still being the cheapest material. Hence bakelite is the clear choice of isolation material. The three revolving shutter materials show different results. Magnesium alloy is expensive and does not perform on the same level as the rest of the materials. The polystyrene breaks because of the low yield limit but might perform good with lower temperatures in the engine. Polystyrene is almost five times more inexpensive than the two other materials. That includes the ABS thermoplastic which because of the 10 % carbon fiber has a high yield limit and does not break like polystyrene or magnesium. Hence the ABS 10 % carbon fiber is the best material. However polystyrene might work with lowered temperature and be a good choice for a low price.

It is clear that the scaled Six Sigma quality approach clarified that there are important improvements that are vital to be solved on the physical model. All the defined GREC problems in this stage are rather comprehensive, for example that the GREC malfunction during its cycle. However with the use of this quality approach the possibility for narrowing down each problem gives insight and information for how the problem could be approached and therefore state a path to an improvement solution. For now the Six Sigma quality approach is rather simple but in the future when the development has gone further and the TRL value has become higher, the whole toolbox of Six Sigma[15] can be considered and used in a way that suits the GREC concept and its technology.

7 References

Articles

(11) Yano, J.-I.; Plant, R. Convective quasi-equilibrium. *Reviews of Geophysics* **2012**, *50*.

(15) Montgomery, D. C.; Woodall, W. H. An overview of six sigma. *International Statistical Review/Revue Internationale de Statistique* **2008**, 329–346.

(16) Bizarro, J. P. The thermodynamic efficiency of heat engines with friction. *American Journal of Physics* **2012**, *80*, 298–305.

Websites

(1) UNFCCC The Paris Agreement `https://unfccc.int/process-and-meetings/the-paris-agreement/the-paris-agreement`.

(3) Tzinis, I. Technology Readiness Level `https://www.nasa.gov/directorates/heo/scan/engine%20ering/technology/technology_readiness_level`.

(4) Karlberg, N. The Revolution Energy Converter explained `https://liuonline-my.sharepoint.com/personal/marer934_student_liu_se/Documents/GREC/Dokument/Projekt%20information/RevolutionEnergyConverterExplained.pdf?CT=1643365170245&OR=ItemsView`.

(5) nilsinside GREC `https://nilsinside.com/nilsinside/Technology-EN.html`.

(6) CDP All Sustainable Development Goals `https://www.cdp.net/en/policy-and-public-affairs/%20sustainable-development-goals/all-sustainable-devel%20opment-goals`.

(12) Benson, T. What is drag? `https://www.grc.nasa.gov/www/k-12/VirtualAero/BottleRocket/airplane/drag1.html`.

(14) Karlberg, N. Brassac GREC Lab Model v2 `https://nilsinside.com/nilsinside/parts.html`.

Books

(7) K.Storck, *Formelsamling i termo- och fluiddynamik*; Instution för ekonimisk och industriell utvekcling, Linköping universitet: 2016.

(8) Gordon J. Van Wylen Richard E. Sonntag, C. B., *Fundamentals of classical thermodynamics*; New York : Wiley, cop. 1994: 1994.

(9) Y.A. Cengel J. Cimbala, R. T., *Fundamentals of Thermal-Fluid Sciences, 5th edition*; McGraw Hill: 2020.

(10) Zohuri, B., *Physics of Cryogenics*; Elsevier: 2018.

(13) Holman, J., *Heat Transfer: Tenth Edition*; McGraw-Hill Education: 2010.

Patents

(2) Karlberg, N. A Working Cylinder for an Energy Converter, WO2013162457A1(Patent), 2013.

8 Appendix

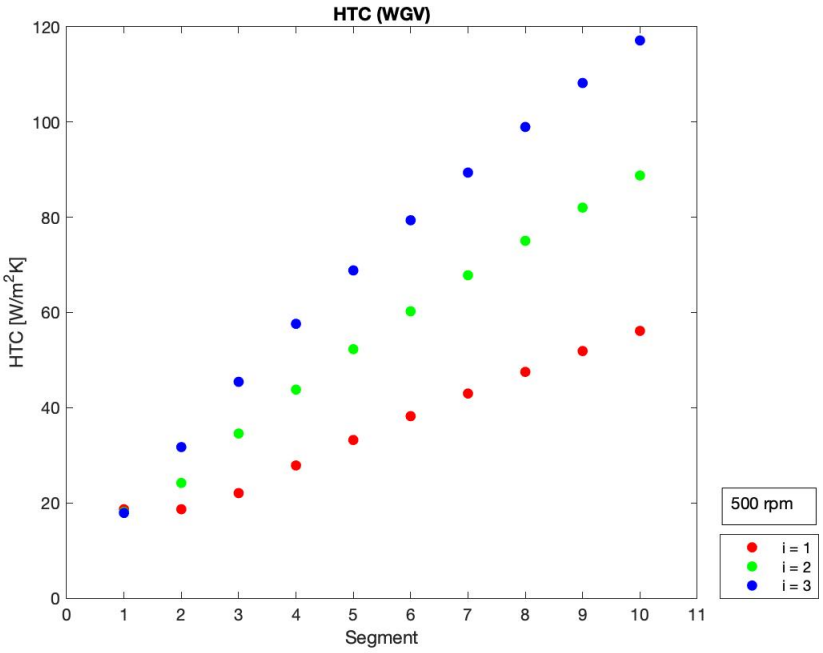

Figure 28: An panoramic view on how the heat transfer coefficient (HTC) changes along the segments in the WGV. The colours represent different scaling of the GREC engine, where the red dots represent the original scaling, the green 2 and the blue 3. The rotation speed used was 500 rpm.

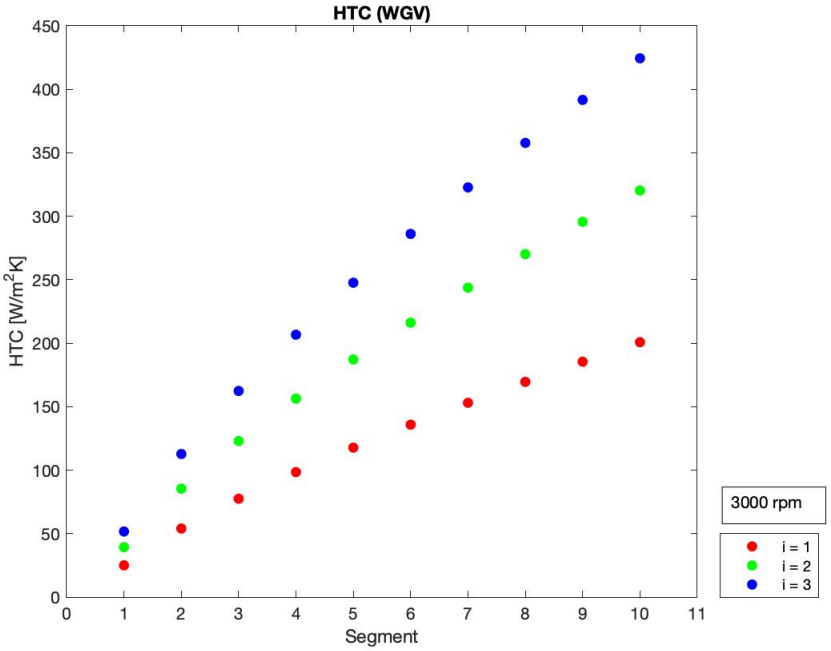

Figure 29: An panoramic view on how the heat transfer coefficient (HTC) changes along the segments in the WGV. The colours represent different scaling of the GREC engine, where the red dots represent the original scaling, the green 2 and the blue 3. The rotation speed used was 3000 rpm.

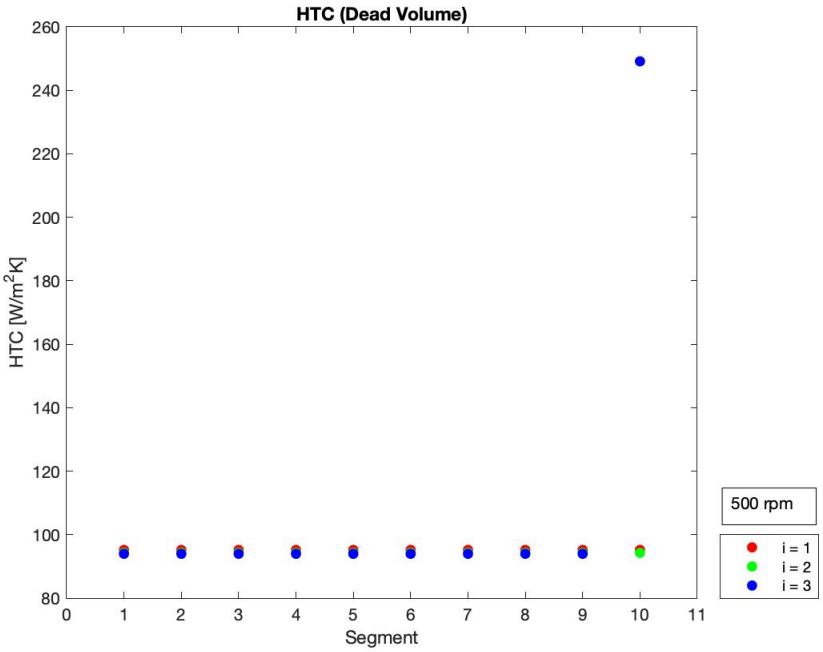

Figure 30: An panoramic view on how the heat transfer coefficient (HTC) changes along the segments in the dead volume. The colours represent different scaling of the GREC engine, where the red dots represent the original scaling, the green 2 and the blue 3.The rotation speed used was 500 rpm.

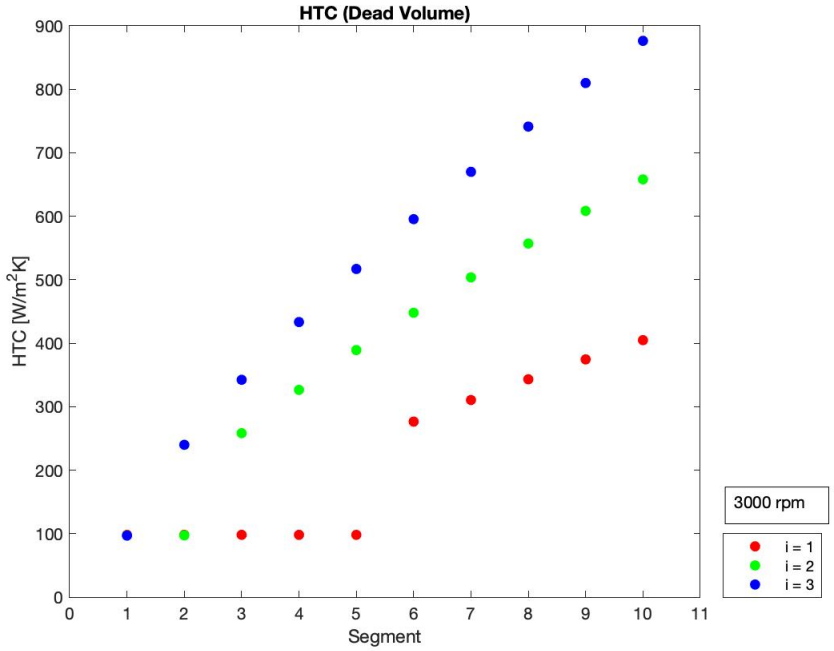

Figure 31: An panoramic view on how the heat transfer coefficient (HTC) changes along the segments in the dead volume. The colours represent different scaling of the GREC engine, where the red dots represent the original scaling, the green 2 and the blue 3.The rotation speed used was 3000 rpm.

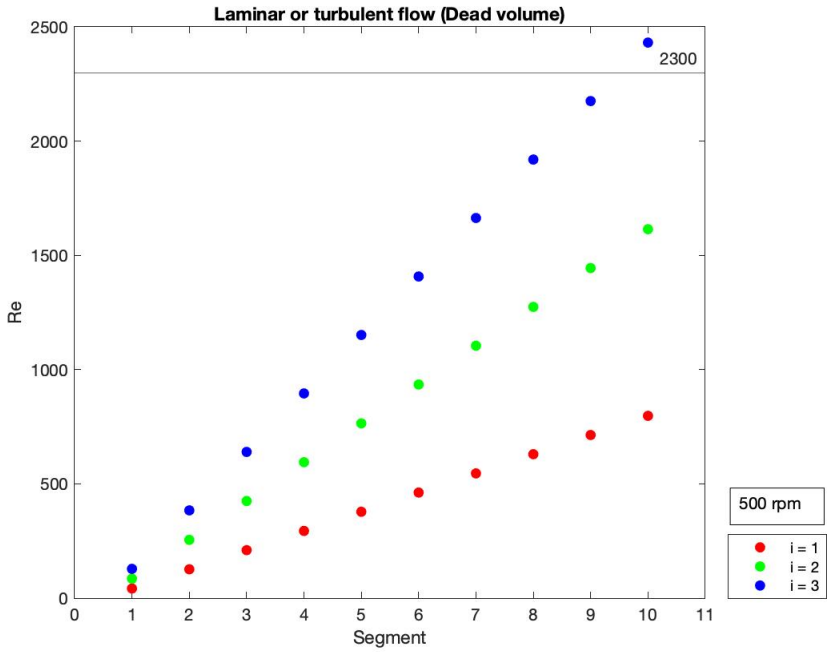

Figure 32: An panoramic view on how the Reynolds number changes along the segments in the dead volume. The colours represent different scaling of the GREC engine, where the red dots represent the original scaling, the green 2 and the blue 3. The black horizontal line is appointed at 2300 and is meant to represent the transit between laminar and turbulent flow. The rotation speed used was 500 rpm.

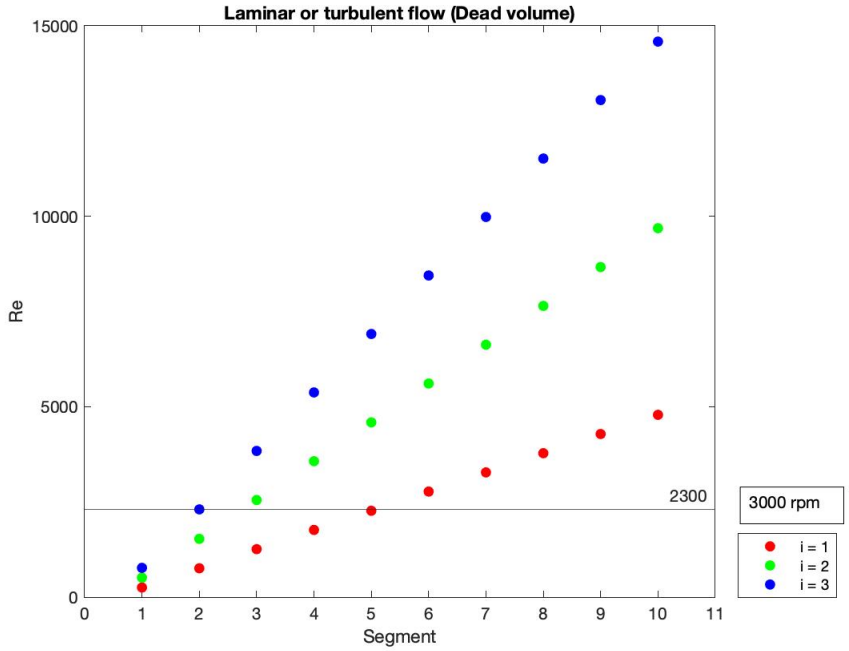

Figure 33: An panoramic view on how the Reynolds number changes along the segments in the dead volume. The colours represent different scaling of the GREC engine, where the red dots represent the original scaling, the green 2 and the blue 3. The black horizontal line is appointed at 2300 and is meant to represent the transit between laminar and turbulent flow. The rotation speed used was 500 rpm.

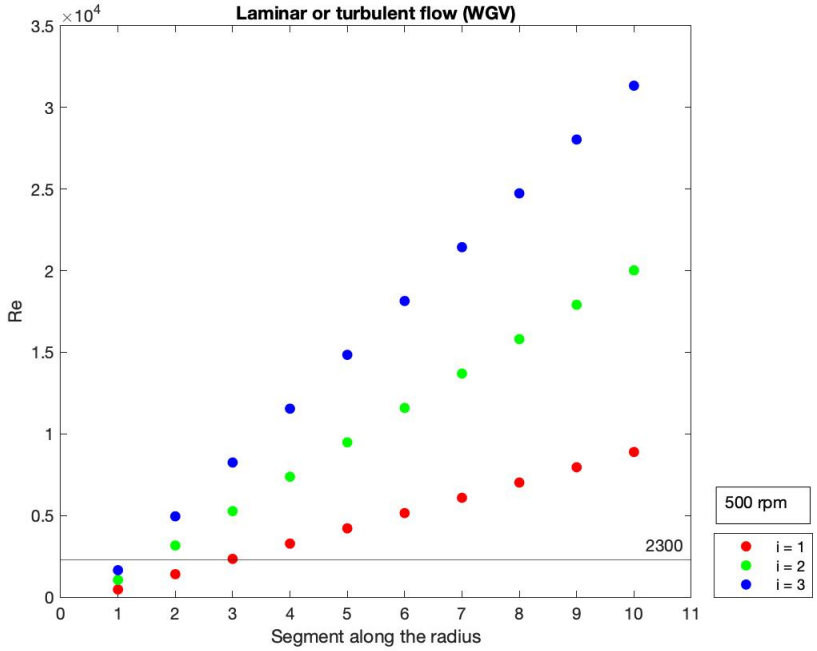

Figure 34: An panoramic view on how the Reynolds number changes along the segments in the WGV. The colours represent different scaling of the GREC engine, where the red dots represent the original scaling, the green 2 and the blue 3. The black horizontal line is appointed at 2300 and is meant to represent the transit between laminar and turbulent flow. The rotation speed used was 500 rpm.

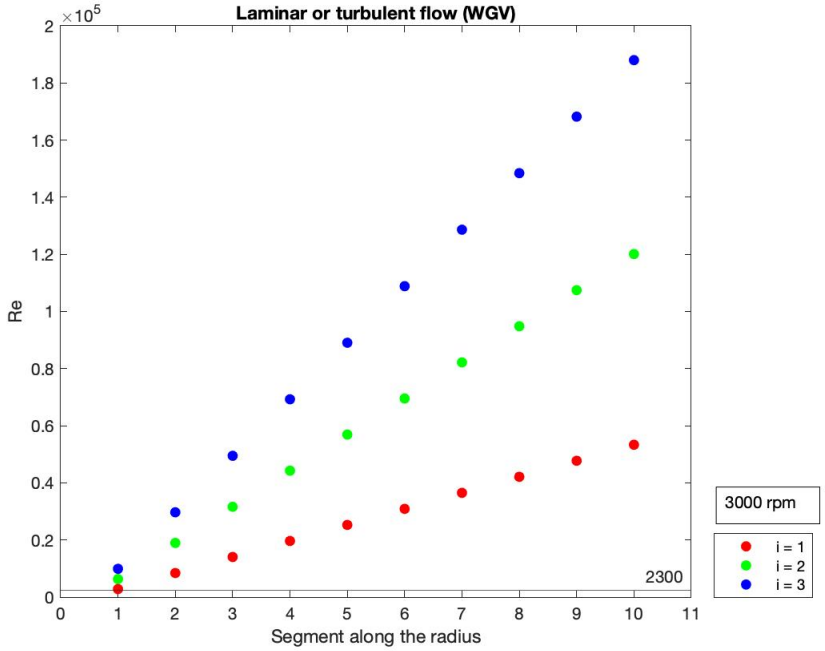

Figure 35: An panoramic view on how the Reynolds number changes along the segments in the WGV. The colours represent different scaling of the GREC engine, where the red dots represent the original scaling, the green 2 and the blue 3. The black horizontal line is appointed at 2300 and is meant to represent the transit between laminar and turbulent flow. The rotation speed used was 3000 rpm.

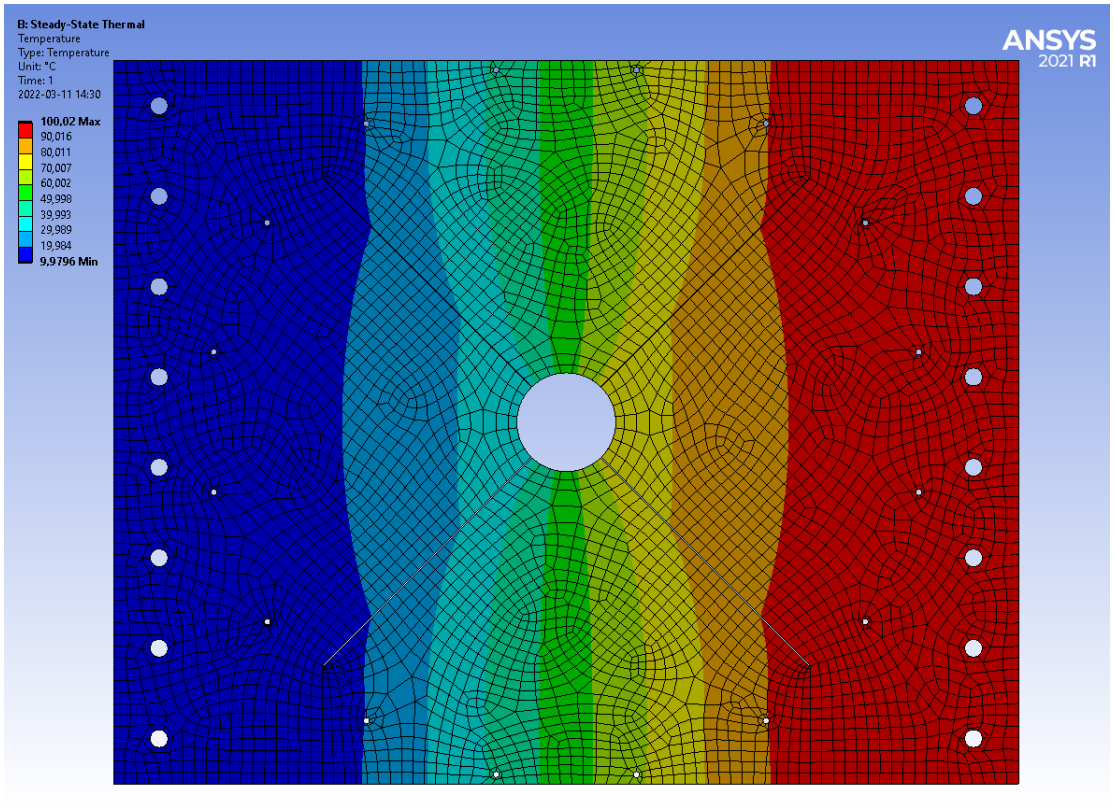

Figure 36: Temperature plot of the copper conducting fin and isolating steel.

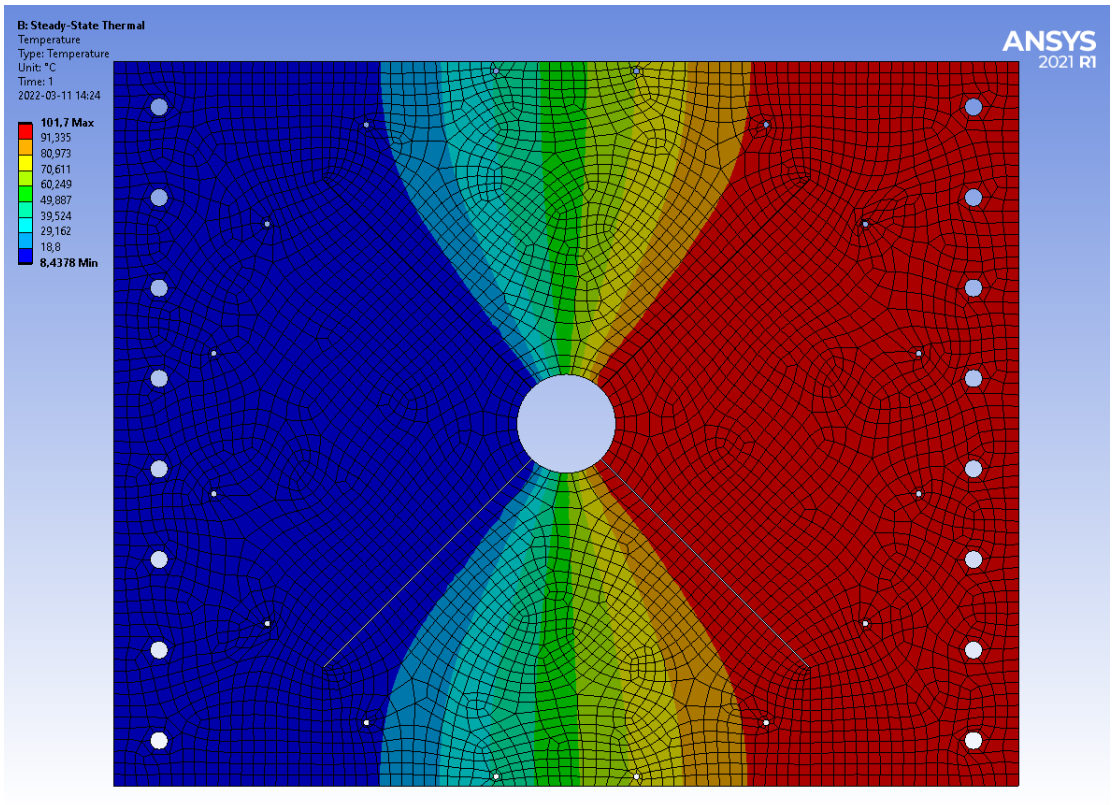

Figure 37: Temperature plot of the copper conducting fin and isolating bakelite.

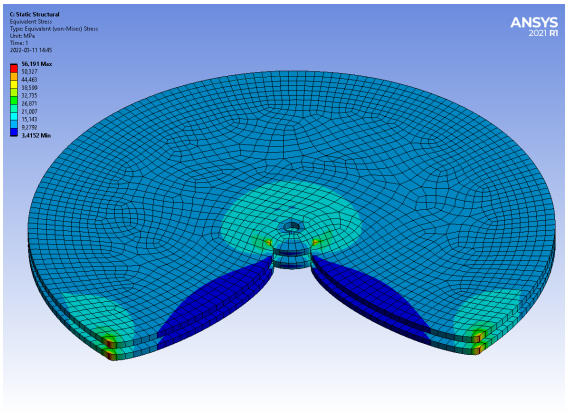

(a) Stress plot for the revolving shutter using ABS 10% carbon fiber.

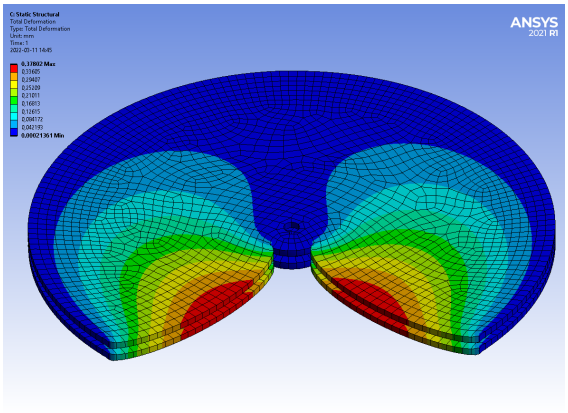

(b) Deformation plot for the revolving shutter using ABS 10% carbon fiber.

Figure 38: Resulting deformation and stress plots from ANSYS for the revolving shutter using ABS 10% carbon fiber.

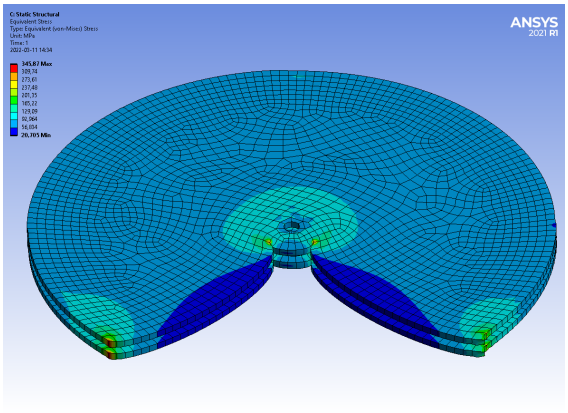

(a) Stress plot for the revolving shutter using magnesium alloy.

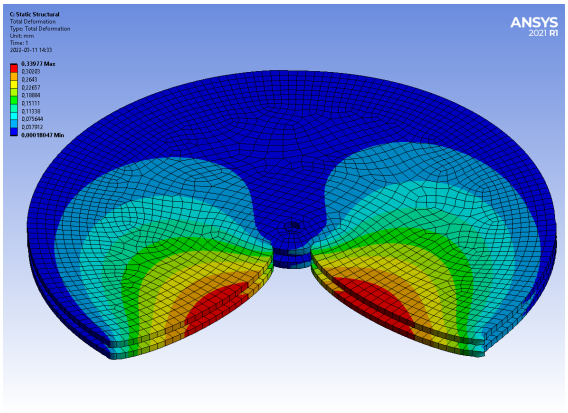

(b) Deformation plot for the revolving shutter using magnesium alloy.

Figure 39: Resulting deformation and stress plots from ANSYS for the revolving shutter using magnesium alloy.

Table 17: How the carnot efficiency changes with an increase of temperature on the heat source.

T_h [°C]	$\eta_{Carnot,th}$[%]
200	40.2
350	54.6
500	63.4

Table 18: Thermal efficiency as a function of rotation speed and scale.

Thermal efficiency [%]			
Scaling / [rpm]	1	2	3
500	7.6	9.8	9.8
1500	6.4	8.0	9.8
3000	6.0	7.2	8.5

Table 19: Total efficiency as a function of rotation speed and scale.

Total efficiency [%]			
Scaling / [rpm]	1	2	3
500	0.1	8.7	9.3
1500	2.3	7.5	9.6
3000	3.3	6.8	8.4

Table 20: How the thermal efficiency changes with an increase of temperature on the heat source.

Thermal efficiency [%]			
Scaling / T_h [°C]	1	2	3
200	13.6	16.5	19.4
350	22.5	26.5	30.1
500	29.8	34.5	39.3

Table 21: How the total efficiency changes with an increase of temperature on the heat source.

Total efficiency [%]			
Scaling / T_h [°C]	1	2	3
200	11.7	16.2	19.3
350	21.4	26.4	30.5
500	29.0	34.4	39.2